

# The influence of chemical composition on models of Type Ia supernovae

Alan C. Calder<sup>1,2,†</sup>, Brendan K. Krueger<sup>1,\*</sup>, Aaron P. Jackson<sup>3</sup>, Dean M. Townsley<sup>4</sup>

<sup>1</sup>*Department of Physics & Astronomy, The State University of New York - Stony Brook, Stony Brook, NY 11794, USA*

<sup>2</sup>*New York Center for Computational Sciences, The State University of New York - Stony Brook, Stony Brook, NY 11794, USA*

<sup>3</sup>*National Research Council Research Associateship Program and Laboratories for Computational Physics and Fluid Dynamics, Naval Research Laboratory, Washington, DC 20375, USA*

<sup>4</sup>*Department of Physics and Astronomy, The University of Alabama, Tuscaloosa, AL 35487, USA*

E-mail: <sup>†</sup>alan.calder@stonybrook.edu

Received December 11, 2012; accepted January 14, 2013

Type Ia supernovae are bright stellar explosions distinguished by standardizable light curves that allow for their use as distance indicators for cosmological studies. Despite the highly successful use of these events in this capacity, many fundamental questions remain. Contemporary research investigates how properties of the progenitor system that follow from the host galaxy such as composition and age influence the brightness of an event with the goal of better understanding and assessing the intrinsic scatter in the brightness. We provide an overview of these supernovae and proposed progenitor systems, all of which involve one or more compact stars known as white dwarfs. We describe contemporary research investigating how the composition and structure of the progenitor white dwarf systematically influences the explosion outcome assuming the progenitor is a single white dwarf that has gained mass from a companion. We present results illustrating some of these systematic effects from our research.

**Keywords** hydrodynamics, nuclear reactions, nucleosynthesis, abundances, stars: supernovae: general, stars: white dwarfs

**PACS numbers** 97.60.Bw, 26.50.+x, 97.20.Rp, 26.30.-k, 95.30.Lz

Contents	4	Research results	178
1 Introduction	168	4.1 Methodology	178
1.1 Historical overview of supernovae	168	4.1.1 Flame model	179
1.2 Observations of Type Ia supernovae	169	4.1.2 Statistical framework	180
1.3 Trends in observations of Type Ia supernovae	170	4.2 Investigation into metallicity	181
1.4 Proposed progenitors systems of Type Ia supernovae	171	4.3 Investigation into central density	181
1.4.1 A single massive white dwarf	171	5 Summary and conclusions	182
1.4.2 Merging white dwarfs	172	Acknowledgements	183
1.4.3 Double detonation models	174	References and notes	183
2 Single degenerate delayed detonation models	175		
3 Contemporary research in the DDT paradigm	175	<b>1 Introduction</b>	
3.1 The role of progenitor composition	175	1.1 Historical overview of supernovae	
3.2 The role of central density	177	“New” or “guest” stars have occasionally appeared in	

\* Presently at CEA Saclay, France

the sky since time immemorial. Ancient observations include solar system objects such as comets and stellar explosions that appear suddenly as a newly visible star. The earliest record of an event associated with a stellar explosion is found in the *The Book of the Later Han* which describes the appearance of a “guest star” in the year 185 [1, 2]. Modern study of stellar explosions began with Tycho Brahe’s naked-eye observations of the event we now call Supernova 1572, and the name “nova” applied to the phenomena of stellar explosions follows from his book *De Stella Nova* (“On the New Star”). Tycho’s observations were of such fidelity that later astronomers were able to reconstruct the light curve and color evolution of this event for comparison and classification [3, 4].

By the early twentieth century, technological advances in astronomy led to recognition of the vast distances to other galaxies, implying that novae observed in other galaxies were in fact extremely bright. This advance, together with advances in theory, resulted in the classification of “super-novae” as bright explosions associated with the violent death of a star (Ref. [5]; see also Refs. [6, 7] for discussion of pioneering work). Observations of a supernova typically produce spectra and a light curve, with spectra taken during the course of an event providing information identifying the constituent elements and the light curve plotting the intensity of light vs. time. As originally proposed by Minkowski [8], supernovae are classified by properties of their spectra and light curves, with the principal distinction arising between events without evidence of hydrogen in their spectra (Type I) and events with evidence of hydrogen in their spectra (Type II). Type I supernovae were further divided into Types Ia, Ib, and eventually Ic [9–12]. The Type Ia sub-classification depends on the observation of a specific Si line [6, 12], not seen in Types Ib and Ic. Type Ib and Ic are distinguished by Type Ib spectra exhibiting He features while Type Ic spectra do not.

Given the extreme brightness of supernovae, only two possible energy sources are thought to account for these phenomena: the release of gravitational potential energy or the release of nuclear binding energy. Events in all of the observational classifications, with the exception of Type Ia, are understood to follow from the gravitational collapses of a massive star that has exhausted its nuclear fuel [13]. The remnant in this type of explosion is a neutron star or black hole, of which many have been observed. Compact remnants have never been observed from Type Ia supernovae. While the classification follows from the spectral signature, Type Ia supernovae are now understood to be the result of a thermonuclear explosion consuming roughly one and a half solar masses of degenerate stellar material composed principally of C

and O [6]. The progenitor systems of these events, however, remain the subject of debate. Most proposed Type Ia progenitor systems follow from the suggestion of Hoyle and Fowler [14] of a thermonuclear runaway occurring in the core of a star supported by electron degeneracy. Various settings in which suitable conditions for the explosive burning of degenerate stellar material have been explored, and scenarios typically involve one or more white dwarf stars, as we discuss below.

## 1.2 Observations of Type Ia supernovae

The release of nuclear binding energy via explosive burning of degenerate C and O provides more than enough kinetic energy to unbind a white dwarf star, and the expansion velocities of freshly synthesized elements typically reach on the order of  $10\,000\text{ km}\cdot\text{s}^{-1}$ . The peak brightness of a Type Ia supernova is set not by the explosion energy, but by the synthesis in the explosion of radioactive  $^{56}\text{Ni}$ , which decays via the chain  $^{56}\text{Ni}$  to  $^{56}\text{Co}$  to  $^{56}\text{Fe}$  releasing photons that power the observed light curve [15–18].

The vast majority of Type Ia supernovae obey a correlation in which the peak brightness is positively correlated with the timescale over which the lightcurve decays from its maximum [19]. This “brighter is broader” trend is known as the Phillips relation [20] and it allows the peak brightnesses to be calibrated so that these events may be treated as “standard candles” for determining distances. The resulting parameter describing the scaling is known as  $\Delta m_{15}(B)$ , which is the change in the apparent  $B$ -band magnitude from peak brightness to 15 days later. The correlation is understood physically as stemming from having both the luminosity and opacity being set by the mass of  $^{56}\text{Ni}$  synthesized in the explosion [21–23]. This relation has been exploited to make Type Ia supernovae the premier distance indicators for cosmological studies. We note that because the galaxy/stellar population is known to have evolved significantly since high ( $z \approx 1$ ) redshifts, the systematics of this evolution must be accounted for to allow precision cosmological measurements. Avoiding relying on empirical relationships is one important goal of the theoretical study of Type Ia supernova explosions.

While the yield of  $^{56}\text{Ni}$  explains the first-order variations in the light curve, current research also aims to understand higher-order effects and the physics behind the Phillips relation. Observations report that Type Ia supernovae appear to have an intrinsic scatter of a few tenths of a magnitude after calibration, forcing a minimum uncertainty in any distances measured by using Type Ia supernovae as standardizable candles [24, 25]. An important goal of theoretical research into Type Ia

supernovae, from the standpoint of cosmology, is to understand the sources of scatter and to identify potential systematic biases by studying the effects of various properties on the mechanism and nucleosynthetic yield of the supernova. The surrounding stellar population and various properties of the progenitor such as its composition, zero-age main sequence mass, thermodynamic state prior to ignition, and cooling and accretion history are known to affect the lightcurves of Type Ia supernovae; the role of these “secondary” parameters is the subject of considerable study (e.g., Refs. [26–28]). Additionally, many of these effects may be interconnected in complex ways [29–32].

### 1.3 Trends in observations of Type Ia supernovae

The interest in Type Ia supernovae that follows from the successful use of these events as distance indicators in studies revealing the acceleration of the Universe [33, 34] has led to modern observational campaigns designed to explore systematic effects on the brightness of these events [35–37]. Observations explore correlations between observed properties of an event such as peak brightness and properties of the host galaxy such as its composition, age, and mass. Many of these galactic properties are correlated, which makes the task of determining the underlying physical reason for correlations between properties of supernovae and their host galaxies difficult. Compounding this difficulty is the fact that detailed observations of galaxies are not available at high redshifts, and parameters (typically galaxy mass and star formation rate) are therefore inferred from galactic models that reproduce the observed spectral energy distribution.

Hamuy *et al.* [38] reported that the peak brightness correlates with the morphological type of the host galaxy, with the most luminous supernovae tending to be hosted by late-type, spiral galaxies. While the trend is striking, supernovae within the same morphological type do not necessarily share the same physical environment. Several physical properties of galaxies tend to correlate with the morphological type. Early-type, elliptical galaxies are thought to form through galaxy mergers and are more massive, contain older stellar populations, and have little star formation. The composition of a galaxy depends largely on the proportion of material that has previously been processed in stars (i.e., elements other than H and He, which are collectively referred to as “metals”). “Metallicity,” the relative abundance of these elements, in the gas phase is correlated with the galaxy mass as galaxies with deeper gravitational potential wells tend to more effectively retain metals [39]. Therefore, early-type galaxies also tend to have higher metallicities. Late-

type, spiral galaxies are less massive, are actively forming stars, and hence contain younger stellar populations. Likely some combination of these properties bias the progenitors of Type Ia supernovae to produce the observed correlation with galaxy morphology.

Despite challenges, Gallagher *et al.* [40] observed a slight dependence of peak brightness on metallicity with dimmer events in metal-rich galaxies. A conclusive trend, however, has proven elusive. Due to the weak correlation with metallicity, progenitor age is suspected to be primarily responsible for variations in the peak brightness [40–43]; however, challenges remain in drawing this conclusion. First, the present gas-phase metallicity of the host galaxy may not be representative of the metallicity of the gas the progenitor star formed from, particularly for older stellar populations. Second, the determination of the age of a stellar population from the integrated light of a galaxy is “degenerate” with the determination of the metallicity [44, 45]. That is, both effects tend to redden the light from a galaxy, so it is difficult to distinguish the true cause of the reddening. For observations of high-redshift galaxies, the metallicity must be inferred from the galaxy mass, precluding the possibility of directly determining its effect on the supernova light curve [43]. When correlations with the inferred stellar population age are considered, dimmer supernovae are found in older populations.

Metallicity could also be responsible for variations in the peak brightness of *calibrated* light curves. At present, observers do not use the Phillips relation [20] but employ much more sophisticated methods to calibrate light curves and thereby measure extragalactic distances. These methods construct calibrated light curves in multiple pass-bands based on templates from nearby events and include corrections for extinction, time dilation, and the K correction for shifting of spectra due to cosmological redshift. Examples include the Spectral Adaptive Light Curve Template SALT [46, 47], the Multicolor Light-Curve Shapes method MLCS2k2 [48, 49], and the (Python-based) supernova light curve fitter SNooPy [50].

Any metallicity dependence reported for calibrated light curves is representative of systematic effects that have not been taken into account in the calibration procedure. Gallagher *et al.* [40, 41] report a dependence in the peak brightness in the calibrated light curves with metallicity, suggesting the possibility of systematic effects with redshift that would have implications on cosmological parameters and the equation of state of dark energy. Howell *et al.* [43], however, using a different calibration method, find no such dependence on metallicity.

Theoretically, the presence of metals in a progenitor white dwarf influences the outcome of the explosion by changing the path of nuclear burning, which influences

the amount of  $^{56}\text{Ni}$  synthesized in an event [51]. Because the decay of  $^{56}\text{Ni}$  powers the light curve, metallicity can therefore directly influence the brightness of an event. Metallicity can also influence the outcome of an explosion in other ways, including changes in the structure of the white dwarf that result from the influence of metallicity on stellar evolution, sedimentation within the white dwarf, the nuclear flame speed, additional sources of opacity, and properties of the thermonuclear burning such as the ignition density (described below) [29, 52].

In addition to properties of the light curves, Type Ia supernovae rates may also yield clues to the progenitors of these explosions. Unlike other types of supernovae, Type Ia have a non-zero rate in older populations, which also points to a white dwarf progenitor. Some results indicate that the dependence of the Ia rate on stellar age is best fit by a bimodal distribution having a prompt component less than 1 Gyr after star formation and a tardy component several Gyr later [53, 54], with the prompt component appearing brighter on average than the tardy component. A bimodal distribution with delay time or mean stellar age would imply two distinct progenitor formation channels. Other studies only indicate a correlation between the delay time and the brightness of Type Ia supernovae favoring a single formation channel, with dimmer events occurring at longer delay times [41–43, 55].

Perhaps the most challenging aspect of observing supernovae is accounting for dust. The process of calibrating light curves and inferring luminosity distances relies on using the width-luminosity relation and color corrections, and the manner in which color is linked to dust is considered controversial [56]. Color variations observed between supernovae correlate with the dust content of the host galaxy, but it is also possible that some of the color variation is intrinsic to properties of the explosion. Observationally disentangling intrinsic variability from effects of dust is the subject of active research [56].

Observations find a surprising range in the variation of the intrinsic brightness of these events, including very bright events that suggest more material burned than could originate from a single white dwarf [57–60]. The logic of observations suggesting that more material burns than could come from a single white dwarf is based on the fact that a white dwarf is supported by electron degeneracy and is therefore subject to a maximum mass, known as the Chandrasekhar limit, beyond which it will collapse to a neutron star [61–63]. A bright observation that suggests more  $^{56}\text{Ni}$  synthesized than the Chandrasekhar maximum mass therefore implies more than one white dwarf was involved. Accordingly, contemporary research explores the efficacy of several progenitor systems with one or more white dwarfs.

## 1.4 Proposed progenitors systems of Type Ia supernovae

We briefly introduce some proposed progenitor systems of Type Ia supernovae and outline contemporary research in each. The accepted result for a Type Ia supernova is an event that produces about  $0.6M_{\odot}$  of  $^{56}\text{Ni}$ , the decay of which produces the light curve, and most models posit the thermonuclear burning of a mix of C and O under degenerate conditions (see Refs. [64, 65], for examples of alternative models). Reviews of progenitor models may be found in Hillebrandt and Niemeyer [6], Livio [66], Wang and Han [67]. While we note that events produce  $0.6M_{\odot}$  of  $^{56}\text{Ni}$ , there is of course scatter in the  $^{56}\text{Ni}$  yield (and brightness) of events and sub-classifications, e.g. Branch-normal, 1998bg-, 1991T-, and 2002cx-like events [68–71].

The association of Type Ia supernovae with white dwarfs began with the work of Hoyle and Fowler [14] who found that the thermonuclear incineration of a mixture of C and O under degenerate conditions could explain Type I supernovae. Hoyle and Fowler [14] theorized a mass approaching the Chandrasekhar limit would be required, but the question remained as to where an appropriate massive stellar core might be found. A suitable progenitor system must satisfy two requirements. First, the system must have enough mass to produce the amount of intermediate-mass and Fe-group elements, e.g.  $^{56}\text{Ni}$ , inferred from observations, a small fraction of which imply more synthesized mass than could come from a single white dwarf. Second, while massive white dwarfs may be composed of mixtures of C and O or O, Ne, and Mg, the progenitors of Type Ia supernovae must be composed principally of C and O because the temperatures required to ignite O or Ne cannot be achieved prior to collapse (see Ref. [72], and references therein). Accordingly, proposed progenitor systems typically involve either multiple C-O white dwarfs or mass transferred from a companion onto a C-O white dwarf.

Many questions concerning progenitor channels remain and are actively being explored as described below. Constraints on progenitor channels are also under study from the perspective of population synthesis (see for example Refs. [73–76]). We note that many questions remain concerning the fundamentals of thermonuclear burning in white dwarf material [77], and, as mentioned above, disentangling the primary from secondary parameters in the observed light curve is a challenge. These many issues influence the question of Type Ia progenitor channels.

### 1.4.1 A single massive white dwarf

This progenitor channel is referred to as a “single degen-



erate” due to the basic requirement that the white dwarf accretes material from a non-degenerate companion such as a red giant, helium, or main sequence star [78] (see also Refs. [79–82]). In fact, the single degenerate channel may be comprised of more than one evolutionary pathway, and several are actively being investigated. While no particular channel has direct observational evidence supporting it, some evolutionary pathways are scrutinized more heavily due to the lack of expected observational features in the light curve and spectra. In particular, a red giant companion to an exploding white dwarf is expected to produce a detectable feature in the UV when the blast wave interacts with the red giant gas [83]. To date, observations of this type of interaction are lacking, which rules out the possibility that the red giant channel is the only evolutionary path. It may still be possible, though, that this pathway contributes a small percentage of the total rate of Type Ia supernovae.

Some specific observations of Branch-normal events provide upper limits of the mass of the companion of those particular systems. For example, the recent SN 2011fe is the closest Type Ia supernova to explode in modern times allowing the earliest time observations as well as detailed pre-explosion images that provide an upper limit to the brightness of the companion star [84, 85]. These observations have ruled out luminous red giants and almost all helium stars as the companion to this particular system [86]. Wheeler [87] has suggested M-dwarfs as a viable donor star due to the expected rates at which WD/M-dwarf binaries are produced; however, further research is needed to explore the unique accretion process that is assisted by the magnetic properties of both the M-dwarf and white dwarf. The evidence in PTF 11kx [88] of nova shells predating the supernova explosion implies that at least some fraction of fairly normal Type Ia supernovae must originate from single degenerate type systems.

The single degenerate W7 model by Nomoto *et al.* [52] that used a parameterized burning velocity offered good agreement with observations and strongly motivated further study of the single degenerate progenitor. The key to the success of W7 follows from the fact that the density at which degenerate stellar material burns largely determines the composition of the ash. At high densities ( $\rho \gtrsim 10^7 \text{g}\cdot\text{cm}^{-3}$ ), nuclear fuel reacts by fusion all the way to the Fe group on the timescale of the burning front propagating through the white dwarf. At lower densities, the burning is incomplete and stops at the Si group or even after C burning. The parameterized reaction of W7 allowed the star to expand prior to the completion of burning, which produced a stratified remnant that agreed well with observations (see Fig. 4 of Ref. [89]).

As the success of the W7 model demonstrates, the nature of the burning in the single degenerate progenitor scenario is critical to the explosion outcome. Arnett [90] investigated C detonations, a case in which burning proceeds as a supersonic front, in the C-O cores of massive stars. The result was that the entire core was incinerated to the Fe group, which is now understood as producing too much Fe. The alternative to a detonation is a deflagration, a subsonic burning front that, in the case of white dwarf material, proceeds by the conductive propagation of heat. Factors such as the interaction of the flame with turbulence influence the burning rate, but after considerable study, the consensus is that a pure deflagration will not produce a normal Type Ia supernova because the relatively slow burning of the deflagration expands the star too much to match observed abundances (see Ref. [91], and references therein).

The favored single degenerate explosion model is that of a period of deflagration (subsonic burning) that allows the star to expand followed by a detonation (supersonic burning) that rapidly incinerates the expanded star. This delayed detonation paradigm was introduced by Khokhlov [92], and simulations of this class of models, like Nomoto’s W7, demonstrate good agreement with observations [93, 94] and have been widely accepted. Many variations on this theme exist, however, including pulsational detonations in which the white dwarf expands and recollapses, subsequently igniting a detonation [94–96], gravitationally confined detonation (GCD) in which compressional heating ignites a detonation in material flowing across the surface of the white dwarf [97, 98] (see also Refs. [99, 100]), and models in which a deflagration transitions to a detonation when the right local conditions are met [92–94, 101–106].

Questions remain about the details of flame ignition: does a localized region initiate explosive burning or is it distributed? If localized regions runaway, how many are there and how are they distributed? Due to the highly nonlinear evolution of the deflagration phase, the details of the ignition process are critically important for determining the outcome of an explosion. At one extreme, single, off-center ignitions likely lead to an asymmetric deflagration phase, like that described in the GCD scenario, while distributed central ignitions lead to fairly symmetric deflagrations. A recent study by Maeda *et al.* [107] suggested that distributed, off-center ignitions produce viewing angle effects that influence the peak brightness, and may be largely responsible for the observed variation.

#### 1.4.2 Merging white dwarfs

The idea of merging white dwarfs as the progenitors of

Type Ia supernovae has been around for some time with investigations into near- and super-Chandrasekhar mass coalesced objects [108–111]. The simplest picture of the merging white dwarf scenario has tidal effects disrupting the secondary, which forms a disk from which the primary subsequently accretes C and O. One of the most commonly cited perils of the merging white dwarf model is that the C will ignite at the edge of the coalesced object, and a flame will burn inward, converting the C-O white dwarf into an O-Ne-Mg white dwarf [112, 113]. Instead of becoming a Type Ia supernova, further accretion leads to the collapse of the white dwarf into a neutron star, a scenario termed “accretion-induced collapse” [114]. Because of this concern, the review of Hillebrandt and Niemeyer [6] dismissed the double degenerate scenario. Such a collapse can be avoided if the accretion rate is low enough ( $< \text{few} \times 10^{-6} M_{\odot} \text{ yr}^{-1}$  [113, 115]) that the heating at the surface of the primary does not ignite the C. Models of violent mergers of white dwarfs (described below) also can avoid an accretion-induced collapse by initiating a detonation of the sub-Chandrasekhar mass primary [116]. Accordingly, there is great interest in demonstrating that the detailed accretion and burning processes provide a mechanism to avoid accretion-induced collapse.

There are a number of studies reported in the literature that have advanced the state of understanding of white dwarf mergers that we highlight here. Other studies investigated collisions of white dwarfs [117–120]. These events may produce Type Ia supernovae, but because the likely locations for such collisions are in the dense cores of globular clusters, these events will be rare, perhaps as few as 10–100 per year in the local ( $z < 1$ ) universe [118]. There is also a core-degenerate merger scenario in which a white dwarf merges with the core of an asymptotic giant branch star (see Ref. [121], and references therein).

Benz *et al.* [122] performed some of the earliest simulations of merging white dwarfs and found that the merger remnant is best described as a hot, rapidly rotating thick disk consisting of the tidally-disrupted secondary surrounding the original primary white dwarf. These simulations confirmed the basic idea that the inspiral of the white dwarfs driven by gravitational radiation can cause the ultimate merger of the system, and emphasized that angular momentum transport is the primary physical mechanism that shapes the outcome.

Yoon *et al.* [123] modeled the merger of  $0.9 M_{\odot}$  and  $0.6 M_{\odot}$  white dwarfs and argued that accurate modeling of the merger event is critical to determining the details of the coalesced remnant. Their simulation indicated the less massive star was disrupted, and the result was described as “a differentially rotating single C-O star

consisting of a slowly rotating cold core and a rapidly rotating hot extended envelope surrounded by a Keplerian disk” instead of the white dwarf and thick disk found in earlier studies. Based on mapping the result of the three-dimensional simulation to one dimension to study burning, they argued that this configuration does not give rise to ignition at the edge of the star and hence the formation of an O-Ne-Mg white dwarf. Instead, central ignition of the C-O remnant can occur.

An extensive study was made by Lorén-Aguilar *et al.* [124], who considered different systems with varying masses. As with the Yoon *et al.* case, they found that the systems avoid igniting the C explosively at the instant of merger. They found a coalesced remnant configuration similar to that of Yoon *et al.*, again consisting of a rotating core, hot envelope (which they term “corona”), and a Keplerian disk. Perhaps owing to different initial conditions, the final core temperatures differed by orders of magnitude between the two groups. Lorén-Aguilar *et al.* [124] concluded that the disks surrounding the remnant are very turbulent, and argued that this would lead to high accretion rates and, subsequently, off-center ignition and accretion induced collapse. Shen *et al.* [125] also find that C does not explosively ignite during the merger, but for different physical reasons owing to the ability of magnetic stresses to redistribute angular momentum. Over a longer timescale after the merger, they find that conditions at the interface of the tidally disrupted secondary and primary white dwarf are such that convective C burning should ensue leading to slow shell burning that eventually results in a high-mass O-Ne-Mg white dwarf or accretion induced collapse.

Other work serves to stress the importance of the fidelity of numerical methods and included physics. Fryer and Diehl [126] and Diehl *et al.* [127] performed simulations of merging white dwarfs with similar methods but found different results. The collaboration of D’Souza *et al.* [128] and [129] with different, grid-based methods found that, depending on the initial configuration, stable mass transfer could be achieved, a result seen only by Fryer and Diehl *et al.* [126]. Recently, Dan *et al.* [130] investigated the issue of stable mass transfer and found it possible with a careful treatment of initial conditions and Dan *et al.* [131] performed a wide-ranging survey, but found the chance of a successful detonation following a merger of C-O white dwarfs small. A nice opus on many of the concerns was produced by Pakmor *et al.* [132].

Recent studies indicate success with white dwarf merger models. Pakmor *et al.* [133] found that the case of nearly equal masses of  $\approx 0.9 M_{\odot}$  may explain sub-luminous events. Pakmor *et al.* [116] found that violent mergers with primary masses of  $\approx 0.9 M_{\odot}$  and mass ra-

tios  $< 0.8$  will produce explosions and are promising candidates for sub-luminous events. Very recently, Pakmor *et al.* [134] found that under the right conditions, the violent merger of two C-O white dwarfs may produce a normal Type Ia supernova.

The merger of two white dwarfs is also thought to possibly produce a rapidly rotating massive white dwarf [135]. Following considerable exploration of detonation scenarios including one-dimensional rotating and off-center models [see Ref. [72], and references therein], the first multidimensional simulations of detonations in rapidly rotating white dwarfs were performed by Steinmetz *et al.* [135]. The result of these two-dimensional simulations indicated that as with earlier studies of detonations [90], the bulk of the star burned all the way to Fe-group elements and did not produce the expected intermediate-mass elements.

Recently, Pfannes *et al.* [136] performed full three-dimensional simulations of turbulent deflagrations in rapidly rotating massive white dwarfs. They found that the amount of burning in their rotating models was similar to that of deflagrations occurring in non-rotating massive white dwarfs, producing “comparably weak and anisotropic explosions that leave behind unburnt material at the center and in the equatorial plane.” The conclusion drawn from their deflagration models is that rotation will not explain the observed variation in peak luminosities. Pfannes *et al.* [137] explored detonations occurring in rapidly rotating massive white dwarfs with three-dimensional simulations. In this case, models indicated that prompt detonations could produce bright supernova-like events, including producing sufficient amounts of intermediate-mass elements. They conclude that detonations in rapidly rotating massive white dwarfs can explain some bright events.

Additional support for the idea that rapidly rotating massive white dwarfs might explain some bright events comes from the recent study of Hachisu *et al.* [138]. They presented a model that includes optically thick winds from an accreting white dwarf, mass stripping from the binary companion by the white dwarf wind, and support from differential rotation. They report that masses can reach up to  $2.7M_{\odot}$  and explored the results of explosions occurring in three mass ranges that depend on the character of the rotation and the onset of secular instability and conclude that the model can explain both bright and normal events, and that differences in angular momentum loss rates (and thus spindown rates) might explain “prompt” and “tardy” components of supernova observations.

### 1.4.3 Double detonation models

Another progenitor channel under study is known as the

“double detonation” model. This idea is similar to the single degenerate scenario described in Section 1.4.1, but in this case the white dwarf does not need to approach the Chandrasekhar limiting mass. Pioneering work introducing double detonation models was performed by Woosley *et al.* [139], Taam [140, 141], and Nomoto [142, 143]. Studies indicated that under the right conditions, an accreted He layer could flash with such strength as to produce an inwardly propagating shock that would ignite a detonation in the C-O core. Studies also indicated that the double detonation scenario could work for a wide range of white dwarf masses, not just the near-Chandrasekhar case [144], and, accordingly, lower mass models were dubbed “sub-Chandrasekhar” [145].

Multidimensional simulations confirmed many of these findings, but as with other models, uncertainties in parts of the problem like the initial conditions were found to play a significant role on the explosion outcome. Accordingly, a common conclusion was that double detonation models may explain some events [94, 146–151]. Most models included a massive He layer  $\sim 0.2M_{\odot}$  so that intermediate and heavy elements synthesized in the He detonation of such models would appear in the outer parts of the ejecta, a result at odds with observations [94, 148, 152, 153].

Recently, however, Bildsten *et al.* [154] found that fairly thin He layers,  $\sim 0.06M_{\odot}$ , could become dynamically unstable and flash on sub-Chandrasekhar mass white dwarfs, and Fink *et al.* [155] found that a He detonation at the base of the accreted layer “robustly triggers” secondary detonations in the C-O core. Kromer *et al.* [156] further investigated the models of Fink *et al.* [155] and calculated light curves. They found the right range of rise and decline times and brightness, but found the color too red due to composition of the He shell ash.

Woosley and Kasen [157] performed an extensive one-dimensional parameter study, calculating nucleosynthesis and light curves for a variety of white dwarf masses and temperatures and He accretion rates. They found that only hot, massive white dwarfs with thin He layers produce Ia-like events and discussed a number of potential objections to these models as a general solution to the Type Ia supernova problem. Sim *et al.* [153] investigated central detonations in bare (no He layer) sub-Chandrasekhar mass C-O white dwarfs. They produced light curves and detailed nucleosynthesis results and concluded that such models are “in qualitatively good agreement with observed properties of Type Ia supernovae,” but note that the question of realistic progenitor systems in keeping with these models remains. Sim *et al.* [158] investigated double detonation scenarios with both edge-lit and central C detonations. They found that for relatively higher mass accreted He shells, conditions are likely for

a core detonation to occur following a He detonation for all expected C-O core masses. The light curves of these core detonation models were readily distinguishable from edge-lit or He detonation with no core detonation models. All these recent studies serve to stress the importance of details of the accreted layer to the distribution of nuclei in the ejecta and the need for high-fidelity spectral observations for validating this class of models.

## 2 Single degenerate delayed detonation models

The single degenerate scenario posits compressional heating of a white dwarf due to accretion. The core of the white dwarf begins runaway heating due to C fusion outpacing neutrino losses [159, 160] and a period of convection ensues [161, and references therein]. When heat generation outpaces transport of heat by convection, a flame is born that eventually will incinerate the white dwarf. The central density at flame ignition is slightly decreased (see, e.g., Piro and Bildsten [162]) and is generally near  $\sim 2 \times 10^9 \text{ g}\cdot\text{cm}^{-3}$  for successful models of Type Ia supernovae (e.g., Refs. [52, 94]).

A variation of the delayed detonation mechanism (within the single degenerate paradigm) is that of a deflagration to detonation transition (DDT). After ignition, the flame propagates as a subsonic deflagration for a while and then transitions to a supersonic detonation that rapidly consumes the star [92–94, 101–106]. We describe the details of our implementation of this explosion mechanism below.

At present, the physical mechanism by which a DDT in degenerate supernova material occurs is an area of current research (see Refs. [163–168], and references therein). Simulations of supernovae involving DDT assume it occurs via the Zeldovich-gradient mechanism (Ref. [103], but see also Refs. [106, 164]), in which a gradient in reactivity leads to a series of explosions that are in phase with the velocity of a steadily propagating detonation wave. Many authors suggest that when the flame reaches a state of distributed burning, which is when turbulence on scales at or below the laminar flame width is fast enough to dominate transport processes (see, e.g., Ref. [169]), fuel and ash are mixed and the temperature of the fuel is raised and “prepared” in such a way to produce the required reactivity gradient. A requirement for distributed burning is that the ratio of turbulent intensity to the laminar flame speed must exceed some unknown threshold, which is still actively researched [103, 104, 170–175]. Entrance into the distributed burning regime does not guarantee such a reactivity gradient to form. Woosley [176] and Woosley *et al.*

[165] studied incorporating more stringent requirements for these conditions to be met.

For burning under conditions found in the white dwarf, the ratio of turbulent intensity to laminar flame speed changes most rapidly due to the change in laminar flame properties, which are strongly dependent on fuel density. Therefore, a DDT is typically assumed to occur at a range of densities that generally lie in the range of  $10^{6.7}$  to  $10^{7.7} \text{ g}\cdot\text{cm}^{-3}$  [103, 176–181], although some research implements DDT criteria that include the strength of background turbulence [28, and references therein]. In simulations, the choice of  $\rho_{\text{DDT}}$  increases or decreases the duration of the deflagration phase, which increases or decreases the amount of expansion prior to the detonation and hence the composition of the yield of Iron Group Elements (IGEs) [181].

## 3 Contemporary research in the DDT paradigm

As outlined above, DDT models agree well with observations and accordingly have been accepted as the favored model of Type Ia supernovae. As the models work well, contemporary research goes well beyond questions of whether or not explosions happen to explore secondary parameters beyond the primary light curve parameter, the brightness or  $\Delta m_{15}(B)$  [27, 28]. In this section, we address the role of composition and central density on the explosion of models of Type Ia supernovae in the single degenerate DDT paradigm.

### 3.1 The role of progenitor composition

The composition of a white dwarf can influence the explosion in a host of ways, including the density at which the deflagration ignites, the flame speed, the density at which the DDT occurs, the energy released during the phases of burning, and the neutron excess of the burned material, which strongly influences properties of the light curve of an event, including the peak brightness, expansion velocities, and the width-luminosity relation. The most important constituents of the progenitor white dwarf are  $^{12}\text{C}$ ,  $^{16}\text{O}$ , and  $^{22}\text{Ne}$ . The composition is principally set by the post-main sequence evolution [29], with the inner core formed during the convective core He-burning phase, and the outer layers formed in shell burning on the asymptotic giant branch [182, and references therein]. These two burning stages operate in very different burning regimes with core He burning occurring at lower temperatures and higher densities than shell burning. At these lower temperatures in the core, the  $^{12}\text{C}(\alpha, \gamma)^{16}\text{O}$  reaction is favored over  $3\alpha$ , and as a result  $^{12}\text{C}$  is depleted in the core, while it is not in the



outer layers [32].

Additionally, the zero-age main sequence (ZAMS) mass and metallicity influence the composition. As the ZAMS mass is increased from the low end of the range that produce C-O white dwarfs, the central temperature is increased during core He burning to favor  $3\alpha$  over  $^{12}\text{C}(\alpha, \gamma)^{16}\text{O}$ , thereby increasing the C/O ratio. As the ZAMS mass continues to increase, however, convection in the core becomes a dominant process in transporting heat away from the core and the competition between  $3\alpha$  and  $^{12}\text{C}(\alpha, \gamma)^{16}\text{O}$  shifts back to favor  $^{12}\text{C}(\alpha, \gamma)^{16}\text{O}$ , resulting in a reduced C/O ratio for the highest ZAMS masses capable of producing CO white dwarfs. The C/O ratio is sensitive to the treatment of the convection process and is still actively researched [29, 32, 182]. Increased metallicity increases the opacity and results in a smaller core mass and lower central temperature, thus mimicking the effects of a decreased ZAMS mass [183]. For a given temperature, increased metallicity also reduces the  $3\alpha$  rate to favor  $^{12}\text{C}$  destruction via  $^{12}\text{C}(\alpha, \gamma)^{16}\text{O}$ , which results in a lower C/O ratio; albeit, the effect is negligible for  $Z < 0.02$  [32].

Neutron rich isotopes are synthesized in two epochs. First, during He burning, the aboriginal C, N, and O is transformed into  $^{22}\text{Ne}$  [51], leading to a direct dependence on metallicity of the parent stellar population. In addition, neutron-rich material is formed in the pre-explosion convective C burning core at a comparable abundance [162, 184].

The density at which the ignition of the deflagration occurs is sensitive to several factors, including  $^{12}\text{C}$  abundance in the core and the thermal history of the core, which follows from the accretion rate and possibly properties of the He flashes [52]. Either of these may have metallicity dependencies involved with both the evolution of the parent stellar population and the still incompletely understood [185] process of progenitor system formation. There are also uncertainties in the screening enhancement of nuclear reactions at these high densities [186, 187], and in the reaction rates themselves, particularly the  $^{12}\text{C} + ^{12}\text{C}$  reaction rate [77, and references therein].

The energy per unit mass released during thermonuclear burning influences both the dynamics of the white dwarf expansion during the deflagration phase and the dynamics of local buoyancy effects that accelerate the flame during the deflagration phase. The composition influences the energy release of thermonuclear burning in two ways. First, the gross nuclear energy available per unit mass is mostly sensitive to the abundance of  $^{12}\text{C}$ . Second, by changing the balance of protons and neutrons, the  $^{22}\text{Ne}$  abundance influences the “ash” to which the material burns, with neutron rich material favoring

more tightly bound nuclei and therefore releasing more energy [188]. The abundances over a broad region of the white dwarf are involved in this case, and, accordingly, involve the products of both the He core and shell burning.

The deflagration propagates via thermal conduction and the laminar flame speed is sensitive to both the  $^{12}\text{C}$  and  $^{22}\text{Ne}$  abundances that influence the energy release and the speed of the early stages of the nuclear fusion [189, 190]. Turbulence from the simmering phase and resulting from buoyancy instability as the flame propagates has the ability to add a nearly arbitrary amount of local area to the flame surface. The effect is to make the burning rate largely independent of the laminar propagation speed [191]. The early deflagration phase, however, when the laminar flame speed interacts with the lower strength turbulence from core convection sets the morphology of the burned region at the point when strong buoyancy effects take over [192].

Although the physics of DDT are incompletely understood, the process will depend on composition because both the flame speed and width depend on the abundances of  $^{12}\text{C}$  and  $^{22}\text{Ne}$ . Depending on the details of the DDT, the transition could occur either in material with the core composition or with the outer layer composition due to the nature of subsonic burning and the response of the star. Figure 1 shows four snapshots of a two-dimensional simulation in which DDT is triggered at a specified density of  $10^{7.1}\text{g}\cdot\text{cm}^{-3}$  (green contour) in a progenitor white dwarf with a different composition in the core than the outer layer (marked by the blue contour). As the deflagration ensues, the star expands and the density contour shrinks. For this transition density, DDT occurs in material from the core, but for lower transition densities, it may be possible for DDT to occur in material from the outer layer. The core  $^{12}\text{C}$  abundance

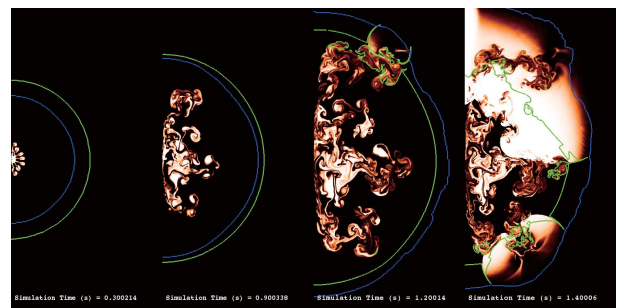


**Fig. 1** A two-dimensional delayed-detonation simulation in which DDT is triggered at a specified density of  $10^{7.1}\text{g}\cdot\text{cm}^{-3}$  shown by the green contour. The core of the progenitor white dwarf is more carbon-depleted than the outer layer with the core-outer layer boundary highlighted with the blue contour. Four different snapshots in time are provided that show the evolution of the flame and the expansion of the white dwarf. Note that the rightmost frame is scaled by a factor of two relative to the others.

will be lower than the outer layer due to the differences in temperature experienced in shell burning as opposed to core He burning. The neutron excess in the core is also expected to be greater than the outer layer due to the slow C burning phase as well as potential sedimentation effects [162, 184, 193–195]. Because the DDT density determines the duration of the deflagration phase and thus degree of expansion of the star at the detonation, the influence of metallicity on the DDT density plays a significant role in the outcome of the explosion [181, 184].

In addition to the indirect effect on energy release described above, the  $^{22}\text{Ne}$  content, which sets the neutron excess, has a direct influence over the final nucleosynthetic products, particularly the amount of  $^{56}\text{Ni}$ . Timmes *et al.* [51] showed that the decrease in the  $^{56}\text{Ni}$  produced in the explosion, absent other factors, should be linearly proportional to the  $^{22}\text{Ne}$  content and therefore the original metallicity of the stellar population, a result seen in some multidimensional results [196]. The distribution of  $^{22}\text{Ne}$  within the white dwarf is important, with  $^{22}\text{Ne}$  in the interior of the star influencing the gross yield and  $^{22}\text{Ne}$  in surface layers influencing the ejecta opacity. Neutron excess also influences the structure of a white dwarf because it is supported by the pressure of degenerate electrons. The neutron excess, determined by the  $^{22}\text{Ne}$  abundance, sets the weight of baryons each electron must support. Accordingly, white dwarfs of a given mass with a higher neutron excess will be more compact because there are fewer total electrons. Conversely, at the same central density, a star with more  $^{22}\text{Ne}$  and thus more neutrons, will be slightly less massive. These concurrent events on the density and structure of the white dwarf may be small [197], but should be included in realistic models due to the marginally bound nature of a near-Chandrasekhar mass white dwarf.

In a comprehensive study using one dimensional DDT models, Höflich *et al.* [105] addressed the influence of initial composition on the nucleosynthesis, light curves, and spectra along with cosmological implications. They found a decreasing C/O ratio released less energy during burning, which increased the duration of the deflagration phase, which in turn decreased the production of  $^{56}\text{Ni}$  and influenced both the bolometric and monochromatic light curves. They also varied the DDT transition density in one model, and found that reduction of the transition density produced similar results on the yield to decreasing the C/O ratio. They reported, however, that there are differences in the distribution of Si in the expanding remnant that lead to slight differences in the light curves. Höflich *et al.* [105] also reported that increasing the metallicity of the progenitor decreased the yield of  $^{56}\text{Ni}$  because the decreased number of protons led to the production of relatively more stable Fe-group

nuclei.

While one-dimensional simulations of Umeda *et al.* [198] also found that a reduced C/O ratio decreased the production of  $^{56}\text{Ni}$ , later three-dimensional deflagration-only simulations by Röpke and Hillebrandt [199] found that the C/O ratio does not significantly influence the final yield of  $^{56}\text{Ni}$ . They attribute this to a complex interplay between the nucleosynthesis and nonlinear turbulent flame evolution. This result was later confirmed with higher resolution simulations and post-processing tracer particles with a more detailed nuclear reaction network [26]; however, due to the highly non-linear nature of the turbulent flame propagation, more simulations with different ignition conditions are necessary to rule out any systematic trend. The effect of the C/O ratio on DDT has yet to be explored in detail; although, Umeda *et al.* [198] speculated that a larger C/O ratio should increase the transition density, and hence, increase the yield of  $^{56}\text{Ni}$ . However, if DDT occurs due to the Zeldovich-gradient mechanism in the distributed burning regime, then the transition density should increase with decreasing C/O ratio because of the stronger effect on the laminar flame properties [181, 190, 200].

The results of Höflich *et al.* [105] contain an important point concerning DDT models we wish to stress. The amount of expansion of the white dwarf during the deflagration phase significantly influences the explosion outcome, particularly the mass of Fe-group elements. We will quantify this result below in the discussion of our research into the the role of the DDT transition density.

Höflich *et al.* [27] addressed secondary parameters of Type Ia supernova light curves, meaning parameters other than  $\Delta m_{15}(B)$ , that influence the brightness of an event. They argued that high quality light curves obtained by the Carnegie Supernova Project [201, 202] show clear evidence of the existence of secondary parameters responsible for variations in the light curves and explored the relationship between possible parameters, central density, the C/O ratio (directly following from the main sequence mass), and metallicity and the light curves from explosion models. The study was based on DDT models with a fixed transition density of  $2.3 \times 10^7 \text{g}\cdot\text{cm}^{-3}$ . They reported that central density and the C/O ratio may be treated as independent secondary parameters characterizing the light curve, and that larger main sequence masses (lower C/O ratios) produces a slower rise of the light curve.

### 3.2 The role of central density

As described above, the composition of the progenitor white dwarf can play an important role in the outcome of an explosion. The composition is determined by many

factors, such as the mass of the main sequence star that became the white dwarf, but it is also influenced by properties of the host galaxy such as metallicity. These properties lead to correlations between galaxy type and brightness of events. A similar property of the progenitor white dwarf that influences the brightness and follows from the age of the progenitor system, and hence the age of the galaxy, is the central density.

As the accreting white dwarf approaches the Chandrasekhar mass, it is relatively insensitive to variations in the central density because of the degenerate equation of state. The configuration of the convecting interior is uncertain, however, because of an incomplete understanding of the physics that influence ignition. There have been many studies of the convective phase [161, 162, 203–208], but examples of remaining uncertainties include the  $^{12}\text{C}$ – $^{12}\text{C}$  rate and its influence on the ignition density [77, 209–211] and the loss of energy due to neutrinos, i.e. the convective Urca process [212–217].

While these many questions remain, it is accepted that the initial mass of the white dwarf (i.e., the mass at which it formed) and the accretion history, particularly the period of cooling prior to the onset of accretion, largely determine the state of the interior of the white dwarf [28]. The study of Lesaffre *et al.* [30] found that white dwarfs experiencing a long cooling period prior to the onset of accretion cool to a lower central temperature, so that once accretion begins to reheat the core a greater increase in density is necessary to reach the conditions for a thermonuclear runaway (see especially Fig. 3 of Ref. [30]). Therefore, while the central density of the white dwarf may have been the same prior to the cooling period, at ignition of the thermonuclear runaway the central density is higher for white dwarfs with a longer cooling time.

The effect of density on electron capture rates has been known for some time [90, and references therein]. Electron capture rates increase with density, so that at the higher densities found in near-Chandrasekhar mass white dwarfs, the rates are rapid enough that significant neutronization occurs during the explosion. The issue of the effect of central density has been explored by many research groups [26–28, 218, 219] and below we highlight some of this work.

Höflich *et al.* [27] in their study of secondary parameters of Type Ia supernova light curves considered central density. They found that the central density influences the later evolution of the light curve ( $\sim 30$  days after maximum and later) with increases in central density causing the later portion of the light curve to shift down and vice versa. They attribute this difference to differences in the amount and distribution of  $^{56}\text{Ni}$  in the central envelope.

Recently Seitenzahl *et al.* [28] explored the effect of changing central density on the explosion outcome with three-dimensional models and a treatment of the energetics of the thermonuclear burning similar to the method we employ (described below) that includes weak interactions, specifically electron capture, allowing their models to neutronize. Seitenzahl *et al.* [28] found that the increased neutronization rates decreased the relative abundance of  $^{56}\text{Ni}$  in the Fe-group material synthesized in the explosion. Considering an identical spatial distribution of ignition kernels, however, they found the increased gravitational acceleration following from a higher central density increases the production of turbulence, which produces a higher burning rate and triggers the DDT sooner, with less expansion of the star and therefore a higher yield of Fe-group elements. These two effects combine to give the relatively constant yield of  $^{56}\text{Ni}$ , and they conclude that the net effect is that the mass of  $^{56}\text{Ni}$  synthesized in an explosion appears insensitive to the central density of the progenitor white dwarf. More recent three-dimensional results including detailed nucleosynthetic post-processing of  $1 \times 10^6$  tracer particles per model suggest that  $^{56}\text{Ni}$  mass increases with central density. In those models, the fraction of  $^{56}\text{Ni}$  of IGEs decreases due to neutronization, but the increase in the total amount in IGE outweighs the decrease due to neutronization [220].

Seitenzahl *et al.* [28] also reported that the  $^{56}\text{Ni}$  yield is sensitive to the initial conditions, which largely determine the behavior of the deflagration phase. They found that a strong deflagration phase following from a many-kernel (larger) ignition region produces a lower yield of  $^{56}\text{Ni}$  primarily because of the increased expansion of the star during the deflagration phase but also due to increased neutronization during the deflagration phase. They note that this confirms previous studies indicating that the strength of the deflagration phase is a primary parameter of  $^{56}\text{Ni}$  production [221].

---

## 4 Research results

In this section we provide a brief summary of our own theoretical research into systematic effects on the brightness of Type Ia supernova explosions. We describe our methodology, including our models and statistical approach to studying systematic effects, and present highlights from our investigation into the role of the metallicity and central density of the progenitor white dwarf. We gratefully acknowledge contributions to the results presented here from our many collaborators.

### 4.1 Methodology

Our methodology for the theoretical study of Type Ia su-

pernovae consists of four principal parts. First is the ability to construct parameterized, hydrostatic initial white dwarf progenitors that can freely change thermal and compositional structure to match features from the literature about progenitor models [181]. Second is a model flame and energetics scheme with which to track both (subsonic) deflagrations and (supersonic) detonations as well as the evolution of dynamic ash in nuclear statistical equilibrium (NSE). This flame/energetics scheme is implemented in the Flash hydrodynamics code [222–224]. Third is utilization of a scheme to post-process the density and temperature histories of Lagrangian tracer particles with a detailed nuclear network in order to calculate detailed nucleosynthetic yields [225, 226]. Fourth, we developed a statistical framework with which to perform ensembles of simulations for well-controlled studies of systematic effects. Below we highlight the flame model and the statistical framework. Complete details of the methodology can be found in previously published results [31, 188, 225–227]. The simulations presented here are all two-dimensional.

#### 4.1.1 Flame model

The significant disparity between the length scale of a white dwarf ( $\sim 10^9$  cm) and the width of laminar nuclear flame ( $< 1$  cm) necessitates the use of a model flame in simulations of Type Ia supernovae. Even simulations with adaptive mesh refinement cannot resolve the actual diffusive flame front in a simulation of the event. The model we use propagates an artificially broadened flame front with an advection-diffusion-reaction (ADR) scheme [228, 229] that has been demonstrated to be acoustically quiet and produce a unique flame speed [227]. This scheme evolves a reaction progress variable  $\phi$ , where  $\phi = 0$  indicates unburned fuel and  $\phi = 1$  indicates burned ash, with the advection-diffusion-reaction equation

$$\partial_t \phi + \vec{u} \cdot \nabla \phi = \kappa \nabla^2 \phi + \frac{1}{\tau} R(\phi) \quad (1)$$

Here  $\kappa$  is a constant and  $R(\phi)$  a non-dimensional function, and both are tuned to propagate the reaction front at the physical speed of the real flame [190, 230] and to be just wide enough to be resolved in our simulation. We use a modified version of the KPP reaction rate discussed by Vladimirova *et al.* [229], in which  $R \propto (\phi - \epsilon)(1 - \phi + \epsilon)$ , where  $\epsilon \simeq 10^{-3}$ , which is acoustically quiet and gives a unique flame speed [227].

In simulating the deflagration phase, the flame front separates expanded burned material (the hot ash) from denser unburned stellar material (cold fuel). The expansion and buoyancy of the burned material forces the in-

terface upward into the denser fuel, and the configuration is susceptible to the Rayleigh–Taylor fluid instability [231, 232]. It is necessary to enhance the flame speed in order to prevent turbulence generated by the Rayleigh–Taylor instability from destroying the artificially broadened flame front. In the simulations discussed here, the enhancement is accomplished by the method suggested by Khokhlov [228] in which we prevent the flame front speed,  $s$ , from falling below a threshold that is scaled with the strength of the Rayleigh–Taylor instability on the scale of the flame front ( $s \propto \sqrt{g\ell}$ , where  $g$  is the local gravity and  $\ell$  is the width of the artificial flame, which is a few times the grid resolution). This scaling of the flame speed prevents the Rayleigh–Taylor instability from effectively pulling the flame apart and also mimics what is a real enhancement of the burning area that is occurring due to structure in the flame surface on unresolved scales. It is expected that, for much of the white dwarf deflagration, the flame is “self-regulated”, in which the small scale structure of the flame surface is always sufficient to keep up with the large-scale buoyancy-driven motions of the burned material. Thus the actual burning rate is determined by this action, which is resolved in our simulations [233].

This technique has demonstrated a suitable level of convergence for studies of Type Ia supernovae [227, 234]. The technique explicitly drops the flame speed to zero below a density of  $10^7$  g·cm $^{-3}$ , approximately where the real flame will be extinguished. This prescription captures some effects of the Rayleigh–Taylor instability and maintains the integrity of the thickened flame, but it does not completely describe the flame-turbulence interaction. Also, we neglect any enhancement from background turbulence from convection prior to the birth of the flame. Future work will include physically-motivated models for these effects [235].

In addition to the model flame, the energetics scheme also includes the nuclear energy release occurring at the flame front, in subsequent burning stages, and in the dynamic ash in nuclear statistical equilibrium. We performed a detailed study of the nuclear processes occurring in a flame in the interior of a white dwarf and developed an efficient and accurate method for incorporating the results into numerical simulations [31, 188, 227]. Tracking even tens of nuclear species is computationally prohibitive, and many more than this are required to accurately calculate the physics such as electron capture rates that are essential to studying rates of neutronization. We instead reproduce the energy release of the nuclear reactions with a highly abstracted model based on tabulation of properties of the burned material calculated in our study of the relevant nuclear processes. This method accurately captures the thermal history of the



material as it burns and evolves, which enables embedded particles to obtain accurate Lagrangian density and temperature histories. Detailed abundances can then be recovered by post-processing these time histories with a nuclear network including hundreds of nuclides.

The nuclear processing can be well-approximated as a three stage process: initially C is consumed, followed by O, which creates a mixture of Si group and light elements that is in quasi-statistical equilibrium, also known as nuclear statistical quasi-equilibrium (NSQE) [236–240]; finally the Si-group nuclei are converted to Fe group, reaching full nuclear statistical equilibrium NSE. In both of these equilibrium states, the capture and creation of light elements (via photodisintegration) is balanced, so that energy release can continue by changing the relative abundance of light (low nuclear binding energy) and heavy (high nuclear binding energy) nuclides, an action that releases energy as buoyant burned material rises and expands. We track each of these stages with separate progress variables and separate relaxation times derived from full nuclear network calculations [188]. We define three progress variables representing consumption of C,  $\phi_C$ , consumption of O to material in NSQE,  $\phi_{\text{NSQE}}$ , and conversion of Si to Fe-group nuclides to form true NSE material,  $\phi_{\text{NSE}}$ . The physical state of the fluid is tracked with the electron number per baryon,  $Y_e$ , the number of nuclei per baryon,  $Y_i$ , and the average binding energy per baryon,  $\bar{q}$ , the minimum properties necessary to hydrodynamically evolve the fluid. C consumption is coupled directly to the flame progress variable,  $\phi_C \equiv \phi$ , from Eq. (1) above, and the later flame stages follow using simple relationships from more detailed calculations.

Burning and evolution of post-flame material change the nuclear binding energy, and we use the binding energy of magnesium to approximate the intermediate burning products of C. The method is finite differenced in such a way to ensure explicit conservation of energy. Weak processes that neutronize the material (e.g. electron capture) are included in the calculation of the energy input rate, as are neutrino losses, which are calculated by convolving the NSE distribution with the weak interaction cross sections. Tracking the conversion of Si-group nuclides to the Fe-group is important for studying the effects of electron capture because the thresholds are lower for the Fe-group nuclides. Both the NSE state and the electron capture rates were calculated with a set of 443 nuclides including all which have weak interaction cross sections given by Langanke and Martínez-Pinedo [241].

Electron capture feeds back on the hydrodynamics in three ways: the NSE can shift to more tightly bound elements as the electron fraction,  $Y_e$ , changes, releasing some energy and changing the local temperature; also

the reduction in  $Y_e$  lowers the Fermi energy, reducing the primary pressure support of this highly degenerate material and having an impact on the buoyancy of the neutronized material; finally neutrinos are emitted (since the star is transparent to them) so that some energy is lost from the system. Also, as we will see below, increased rates of neutronization produce yields of more neutron rich material and therefore less  $^{56}\text{Ni}$ , thereby influencing the brightness of an event. Complete details of the NSE calculations may be found in Ref. [242] and the details of the implementation in our simulations may be found in Ref. [31], Ref. [188], and Ref. [227].

In addition to all of these effects during the deflagration phase of Type Ia supernovae, the progress-variable-based method has been extended to model the gross features of detonations [226, 243]. Instead of coupling the first burning stage,  $\phi_C$ , representing C consumption, to the ADR flame front, we instead can use the actual temperature-dependent rate for C burning, or possibly a more appropriate effective rate. Doing so allows shock propagation to trigger burning and therefore create a propagating detonation. This method has been used successfully by Ref. [244] in modern studies of the DDT, and our multistage burning model shares many features with theirs (see also Refs. [92, 245]). We treat the later burning stages very similarly, though we have taken slightly more care to track the intermediate stages and have nearly eliminated acoustic noise when coupling energy release to the flame.

#### 4.1.2 Statistical framework

We also developed a theoretical framework for the study of systematic effects in Type Ia supernovae [31]. This framework allows the evaluation of the average dependence of the properties of supernovae on underlying parameters, such as composition, by constructing a theoretical sample based on a probabilistic initial ignition condition. Such sample-averaged dependencies are important for understanding how Type Ia models may explain features of the observed sample, particularly samples generated by large dark energy surveys utilizing Type Ia supernovae as distance indicators.

The theoretical sample is constructed to represent statistical properties of the observed sample of Type Ia supernovae such as the mean inferred  $^{56}\text{Ni}$  yield and variance. Within the DDT paradigm, the variance in  $^{56}\text{Ni}$  yields can be explained by the development of fluid instabilities during the deflagration phase of the explosion. By choice of the initial configuration of the flame, we may influence the growth of these fluid instabilities resulting in varying amounts of  $^{56}\text{Ni}$  synthesized during the explosion. In Ref. [31], Townsley *et al.* found that perturbing

a spherical flame surface with radius ( $r_0 = 150$  km) with spherical harmonic modes ( $Y_l^m$ ) between  $12 \leq l \leq 16$  with random amplitudes ( $A$ ) normally distributed between 0–15 km and, for three-dimensional simulations, random phases ( $\delta$ ) uniformly distributed between  $-\pi$ – $\pi$  best characterized the mean inferred  $^{56}\text{Ni}$  yield and sample variance from observations:

$$r(\theta) = r_0 + \sum_{l=l_{\min}}^{l_{\max}} A_l Y_l(\theta) \quad (2)$$

$$r(\theta, \phi) = r_0 + \sum_{l=l_{\min}}^{l_{\max}} \sum_{m=-l}^l \frac{A_l^m e^{i\delta_l^m}}{\sqrt{2l+1}} Y_l^m(\theta, \phi) \quad (3)$$

With a suitable random-number generator, a sample population of progenitor white dwarfs is constructed by defining the initial flame surface for a particular progenitor.

#### 4.2 Investigation into metallicity

We investigated the direct effect of reprocessed stellar material (metals) in the host galaxy via the initial neutron excess of the progenitor white dwarf in Ref. [31]. Because of weak interactions, metals produced by nuclear burning are more neutron rich than H and He, and, accordingly, the neutron excess of these elements is thought to drive the explosion yield toward stable Fe-group elements. Thus, there is relatively less radioactive  $^{56}\text{Ni}$  in the NSE mix, which results in a dimmer event [51]. We investigated this effect by introducing  $^{22}\text{Ne}$  into the progenitor white dwarf as a proxy for (neutron-rich) metals. The presence of  $^{22}\text{Ne}$  influences the progenitor structure, the energy release of the burn, and the flame speed. The study was designed to measure how the  $^{22}\text{Ne}$  content influences the competition between rising plumes and the expansion of the star, which determines the yield. We performed a suite of 20 DDT simulations varying only the initial  $^{22}\text{Ne}$  in a progenitor model, and found a negligible effect on the pre-detonation expansion of the star and thus the yield of NSE material. The neutron excess sets the amount of material in NSE that favors stable Fe-group elements over radioactive  $^{56}\text{Ni}$ . Our results were consistent with earlier work calculating the direct modification of  $^{56}\text{Ni}$  mass from initial neutron excess [51].

In Ref. [181], Jackson *et al.* expanded the earlier study [31] to include the indirect effect of metallicity in the form of the  $^{22}\text{Ne}$  mass fraction through its influence on the density at which the DDT takes place. We simulated 30 realizations each at 5 transition densities between  $(1-3) \times 10^7 \text{ g cm}^{-3}$  for a total of 150 simulations. We found a quadratic dependence of the NSE yield on the log of the transition density, which is determined by the competition between rising unstable plumes and stellar

expansion. By then considering the effect of metallicity on the transition density, we found the NSE yield decreases slightly with metallicity, but that the ratio of the  $^{56}\text{Ni}$  yield to the overall NSE yield does not change as significantly. Observations testing the dependence of the yield on metallicity remain somewhat ambiguous, but the dependence we found is comparable to that inferred from [200]. We also found that the scatter in the results increases with decreasing transition density, and we attribute this increase in scatter to the nonlinear behavior of the unstable rising plumes.

Figure 2 illustrates these results by plotting mass of  $^{56}\text{Ni}$  vs. metallicity for our models and the observational results of Konishi *et al.* [246]. The constant DDT density results (blue curve) represent the direct effect of introducing  $^{22}\text{Ne}$  into the progenitor white dwarf as a proxy for (neutron-rich) metals. The red curves present results adapted from Jackson *et al.* [181] that include the indirect effect of metallicity influencing DDT density. The results inferred from Konishi *et al.* [246] are the black points. In the plot, metallicity is quantified by comparing the ratios of Fe to H in the progenitor white dwarfs relative to our Sun [247]. We write this relationship as

$$[\text{Fe}/\text{H}] \equiv \log_{10} \left[ \frac{(N_{\text{Fe}}/N_{\text{H}})_{\text{star}}}{(N_{\text{Fe}}/N_{\text{H}})_{\text{Sun}}} \right]$$

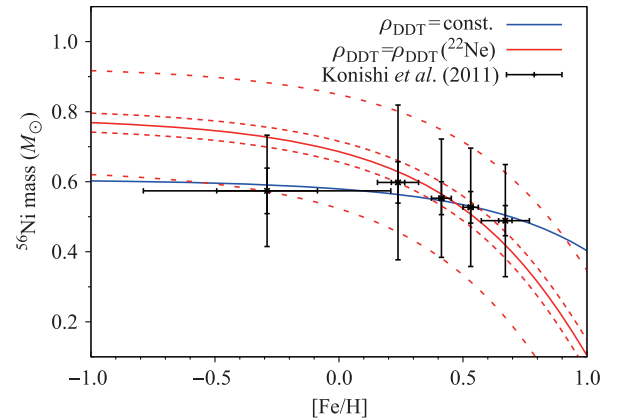


**Fig. 2** Plot of mass of  $^{56}\text{Ni}$  vs. metallicity comparing simulations that varied DDT densities with metallicity to the observational results of Konishi *et al.* [246] (black points). The constant DDT result, blue curve, assumed that the DDT density did not vary with metallicity but included other metallicity effects on the structure of the progenitor star. The red curves present results from adapted from Jackson *et al.* [181], with the solid curve presenting the average value of simulations at a given metallicity and the widely-spaced dashed and dashed curves representing standard deviation and standard error, respectively.

#### 4.3 Investigation into central density

We investigated the effect of central density on the explosion yield in Krueger *et al.* [248]. While we found little change in the overall production of NSE material, we

found a definite trend of decreasing  $^{56}\text{Ni}$  production with increasing progenitor central density. We attribute this result to higher rates of weak interactions (electron captures) that produce a higher proportion of neutronized material at higher density. More neutronization means less symmetric nuclei like  $^{56}\text{Ni}$ , and, accordingly, a dimmer event. This result may explain the observed decrease in Type Ia supernova brightness with increasing delay time. The central density of the progenitor is determined by its evolution, including the transfer of mass from the companion. If there is a long period of cooling before the onset of mass transfer, the central density of the progenitor will be higher when the core reaches the C ignition temperature [30], thereby producing less  $^{56}\text{Ni}$  and thus a dimmer event. In addition, we found considerable variation in the trends from some realizations, stressing the importance of statistical studies.

In Krueger *et al.* [249] we expanded our earlier investigation into the role of central density on the production of  $^{56}\text{Ni}$  and hence the brightness of an event. We presented the details of our models, and found that the distribution of  $^{56}\text{Ni}$  in our models typically shows a somewhat clumpy concentration in the inner region of the remnant, with some dependence of the morphology on the central density. We found a trend of a shortened period of deflagration at higher central densities, but owing to increased rates of neutronization, the total neutronization is greater at higher densities, which explains our trend of decreasing  $^{56}\text{Ni}$  production with increasing progenitor central density. We also considered main sequence evolution in comparing the masses of  $^{56}\text{Ni}$  produced to observations thereby obtaining an improved brightness-age relation from our results.

Figure 3 presents results adapted from Krueger *et al.* [249] relating the results to observations. The principal result of a simulation is the mass of  $^{56}\text{Ni}$  produced, which is directly related to the brightness of an event. Using the method outlined in Ref. [43], we can convert  $^{56}\text{Ni}$  masses to stretch values, a measure related to peak brightness [250], for a more direct comparison with observations. We combined the central density values with the results of Lesaffre *et al.* [30], which correlate the central density at the time of the ignition of the flame front to the cooling time of the progenitor WD (that is, the period of isolation prior to the onset of accretion), allowing us to express our results as ages. The results of Lesaffre *et al.* [30] suggest that a WD with a central density of  $1 \times 10^9 \text{ g}\cdot\text{cm}^{-3}$  will not ignite without further accretion, so for this comparison simulations with that value of central density were neglected. We also applied a shift to our data to account for the main sequence age,  $\tau_{\text{MS}}$ , which we take to be constant across our results. We consider two estimated limiting values for  $\tau_{\text{MS}}$  (0.05 and 1.0 Gyr,

corresponding to main-sequence masses of approximately 8.0 and 1.5 solar masses, respectively; see Hansen *et al.* [251]) and included them with the original  $\tau_{\text{MS}} = 0$  result in Fig. 3. Adding in a  $\tau_{\text{MS}}$  consistent with our C-O progenitors brings our results into better agreement with the two right-most points of Neill *et al.* [42].

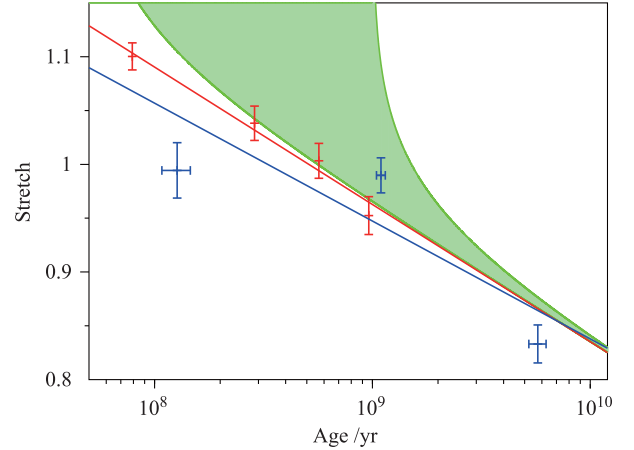


**Fig. 3** Plot of stretch vs. age comparing the scaled results of simulations varying the central density of the progenitor white dwarf to the observations of Neill *et al.* [42]. In red are the points from this study with no shift (i.e.,  $\tau_{\text{MS}} = 0$  Gyr), along with the standard error of the mean and a best-fit trend line. The green shaded region shows our best-fit line with  $\tau_{\text{MS}} = 0.05\text{--}1.0$  Gyr. In blue are the binned and averaged points from Fig. 5 of Neill *et al.* [42], along with their best-fit trend line. Adapted from Ref. [249].

Figure 3 shows that our theoretical results are not in complete agreement with the observed data. Observationally, the age-brightness correlation may flatten at young ages, while our data do not, resulting in our data being too bright relative to young Type Ia supernovae. This study isolated the effects of central density and related that to age assuming a constant main-sequence mass, but there are other effects that may be correlated. Examples of such potentially correlated effects are: main-sequence mass and its correlation with central density, metallicity of the progenitor, core  $^{12}\text{C}$  fraction prior to ignition of the deflagration, sedimentation, and others. Inclusion of such effects may modify the results presented here and are the subjects of future work.

## 5 Summary and conclusions

We have presented an overview of Type Ia supernova explosion models currently under study and a brief description of contemporary research. Both observations and theoretical models are at a level of sophistication that allows comparison at a far more detailed level than just bulk properties such as energy release or bolometric light curve. Instead, studies explore secondary parameters of light curves and the role of properties such as the

age and composition of the progenitor system on the explosion yield and light curve. The structure and composition of a white dwarf follow from properties of the host galaxy such as metallicity and age, and both theorists and observers are able to study trends of brightness with host galaxy type. These studies will better inform future observational campaigns probing the expansion history of the Universe and the properties of dark energy.

Certainly, however, the problem is far from solved. The problems of discerning the progenitor systems(s) and explaining the diversity of events remain. Researchers are actively exploring multiple progenitor systems, to explain “normal” events as well as outliers, both dim and bright. Modeling explosions in these progenitor systems is a challenging problem, necessitating the development of complex sub-grid-scale models, and fundamental questions remain about models and the basic physics therein, e.g. the unsolved problem of turbulent combustion. Good progress is being made, however, and our assessment is that many of the outstanding questions will be answered in the near future.

We presented results from our research into systematic effects on the production of  $^{56}\text{Ni}$  and hence the brightness of an event. Our simulations assume the single degenerate progenitor system and that the explosion proceeds via a DDT. Our approach to studying systematic effects is via suites of simulations allowing quantification of statistical properties. One important result from our research we stress here is the need for a statistical approach to discerning trends as illustrated by the relatively large standard deviation in Fig. 2.

Our models that include the direct effect of metallicity indicate a weak trend of decreasing brightness with increasing metallicity that is consistent with earlier results [51]. Models including the indirect effect of metallicity on flame speeds and the deflagration to detonation transition density demonstrate a significantly stronger trend of decreasing brightness with increasing metallicity. Our results indicate a quadratic dependence of the yield of  $^{56}\text{Ni}$  on the log of the transition density. Relating metallicity to the transition density gave relationship between brightness and metallicity [181].

We also presented results from our research into the effect of central density. Our suites of simulations showed a strong trend of decreasing brightness with increasing central density that we attribute to increase rates of neutronization. Relating our central density results to the age of the progenitor system allows comparison to observations, and in so doing we were able to provide a theoretical explanation of the observed trend that Type Ia supernovae from older host galaxies are systematically dimmer [249]. The agreement between our trend and the observational trends is not perfect, however,

and we recognize that uncertainties abound and our two-dimensional models are incomplete. Plans for the future include targeted three-dimensional simulations including more complete physics to confirm our results.

Our conclusion is that this is an exciting time to be studying the complex problem of thermonuclear supernovae. Substantial progress is being made by both observers and theorists, and we hope that this review of one part of the problem, the role of chemical composition on explosion models, conveys some of this excitement. In preparing this review, we were struck by the remarkable progress that has been made in modeling this complex, multi-scale, multi-physics problem by many talented scientists. We also hope this review conveys our enthusiasm and respect for all of the careful study, both past and present, of the problem of Type Ia supernovae.

**Acknowledgements** This work was supported by the Department of Energy through grants DE-FG02-07ER41516, DE-FG02-08ER41570, and DE-FG02-08ER41565, and NASA through grant NNX09AD19G. ACC also acknowledges support from the Department of Energy under grant DE-FG02-87ER40317. DMT received support from the Bart J. Bok fellowship at the University of Arizona. This research was performed while APJ held a National Research Council Research Associateship Award at the Naval Research Laboratory. The authors also acknowledge the hospitality of the KITP, which is supported by NSF grant PHY05-51164, during the programs “Accretion and Explosion: The Astrophysics of Degenerate Stars” and “Stellar Death and Supernovae”. The software used in this work was in part developed by the DOE-supported ASC/Alliances Center for Astrophysical Thermonuclear Flashes at the University of Chicago. This research utilized resources at the New York Center for Computational Sciences at Stony Brook University/Brookhaven National Laboratory which is supported by the U.S. Department of Energy under Contract No. DE-AC02-98CH10886 and by the State of New York. The authors gratefully thank Ivo Seitenzahl, Max Katz, and Michal Simon for helpful comments on drafts of this manuscript. The authors also thank the anonymous referee for insightful comments and suggestions that significantly improved the manuscript.

## References and notes

1. R. Stothers, *Isis. Journal of the History of Science Society*, 1977, 68: 443
2. L. A. Marschall, *The Supernova Story*, New York: Plenum Press, 1988: 313
3. W. Baade, *Astrophys. J.*, 1945, 102: 309
4. P. Ruiz-Lapuente, *Astrophys. J.*, 2004, 612(1): 357
5. W. Baade and F. Zwicky, *Phys. Rev.*, 1934, 46(1): 76
6. W. Hillebrandt and J. C. Niemeyer, *Ann. Rev. Astron. Astrophys.*, 2000, 38(1): 191
7. D. E. Osterbrock, in: *American Astronomical Society Meeting Abstracts*, *Bull. Am. Astron. Soc.*, 2001, 33: 1330
8. R. Minkowski, *Publ. Astron. Soc. Pac.*, 1941, 53: 224
9. F. Bertola, *Annales d’Astrophysique*, 1964, 27: 319
10. A. C. Porter and A. V. Filippenko, *Astron. J.*, 1987, 93: 1372



11. R. P. Harkness and J. C. Wheeler, in: *Supernovae*, edited by A. G. Petschek, 1990: 1
12. A. V. Filippenko, *Ann. Rev. Astron. Astrophys.*, 1997, 35(1): 309
13. S. A. Colgate and R. H. White, *Astrophys. J.*, 1966, 143: 626
14. F. Hoyle and W. A. Fowler, *Astrophys. J.*, 1960, 132: 565
15. T. Pankey, Jr, Possible Thermonuclear Activities in Natural Terrestrial Minerals., Ph.D. thesis, Howard University, 1962
16. S. A. Colgate and C. McKee, *Astrophys. J.*, 1969, 157: 623
17. S. A. Colgate, A. G. Petschek, and J. T. Kriese, *Astrophys. J.*, 1980, 237: L81
18. M. J. Kuchner, R. P. Kirshner, P. A. Pinto, and B. Leibundgut, *Astrophys. J.*, 1994, 426: L89
19. I. P. Pskovskii, *Sov. Astron.*, 1977, 21: 675
20. M. M. Phillips, *Astrophys. J.*, 1993, 413: L105
21. W. D. Arnett, *Astrophys. J.*, 1982, 253: 785
22. P. A. Pinto and R. G. Eastman, *Astrophys. J.*, 2000, 530(2): 744
23. D. Kasen and S. E. Woosley, *Astrophys. J.*, 2007, 656(2): 661, arXiv: astro-ph/0609540
24. G. H. Jacoby, D. Branch, R. Ciardullo, R. L. Davies, W. E. Harris, M. J. Pierce, C. J. Pritchett, J. L. Tonry, and D. L. Welch, *Publ. Astron. Soc. Pac.*, 1992, 104: 599
25. R. P. Kirshner, arXiv: 0910.0257, 2009
26. F. K. Röpke, M. Gieseler, M. Reinecke, C. Travaglio, and W. Hillebrandt, *Astron. Astrophys.*, 2006, 453: 203, arXiv: astro-ph/0506107
27. P. Höflich, K. Krisciunas, A. M. Khokhlov, E. Baron, G. Folatelli, M. Hamuy, M. M. Phillips, N. Suntzeff, and L. Wang, *Astrophys. J.*, 2010, 710(1): 444, arXiv: 0912.2231
28. I. R. Seitenzahl, F. Ciaraldi-Schoolmann, and F. K. Röpke, *Mon. Not. R. Astron. Soc.*, 2011, 414(3): 2709, arXiv: 1012.4929 [astro-ph.SR]
29. I. Domínguez, P. Höflich, and O. Straniero, *Astrophys. J.*, 2001, 557(1): 279, arXiv: astro-ph/0104257
30. P. Lesaffre, Z. Han, C. A. Tout, P. Podsiadlowski, and R. G. Martin, *Mon. Not. R. Astron. Soc.*, 2006, 368: 187, arXiv: astro-ph/0601443
31. D. M. Townsley, A. P. Jackson, A. C. Calder, D. A. Chamulak, E. F. Brown, and F. X. Timmes, *Astrophys. J.*, 2009, 701(2): 1582, arXiv: 0906.4384 [astro-ph.SR]
32. X. C. Meng and W. M. Yang, *Astron. Astrophys.*, 2011, 531: A94, arXiv: 1105.2860 [astro-ph.SR]
33. A. G. Riess, A. V. Filippenko, P. Challis, A. Clocchiatti, et al., *Astronom. J.*, 1998, 116: 1009, arXiv: astro-ph/9805201
34. S. Perlmutter, G. Aldering, G. Goldhaber, R. A. Knop, et al., *Astrophys. J.*, 1999, 517: 565, arXiv: astro-ph/9812133
35. M. Sullivan, D. Le Borgne, C. J. Pritchett, A. Hodsman, et al., *Astrophys. J.*, 2006, 648(2): 868, arXiv: astro-ph/0605455
36. M. Sullivan, A. Conley, D. A. Howell, J. D. Neill, et al., *Mon. Not. R. Astron. Soc.*, 2010, 406: 782, arXiv: 1003.5119 [astro-ph.CO]
37. W. Li, R. Chornock, J. Leaman, A. V. Filippenko, D. Poznanski, X. Wang, M. Ganeshalingam, and F. Mannucci, *Mon. Not. R. Astron. Soc.*, 2011, 412(3): 1473, arXiv: 1006.4613 [astro-ph.SR]
38. M. Hamuy, M. M. Phillips, N. B. Suntzeff, R. A. Schommer, J. Maza, and R. Avilés, *Astron. J.*, 1996, 112: 2398, arXiv: astro-ph/9609062
39. C. A. Tremonti, T. M. Heckman, G. Kauffmann, J. Brinchmann, S. Charlot, S. D. M. White, M. Seibert, E. W. Peng, D. J. Schlegel, A. Uomoto, M. Fukugita, and J. Brinkmann, *Astrophys. J.*, 2004, 613: 898, arXiv: astro-ph/0405537
40. J. S. Gallagher, P. M. Garnavich, P. Berlind, P. Challis, S. Jha, and R. P. Kirshner, *Astrophys. J.*, 2005, 634(1): 210, arXiv: astro-ph/0508180
41. J. S. Gallagher, P. M. Garnavich, N. Caldwell, R. P. Kirshner, S. W. Jha, W. Li, M. Ganeshalingam, and A. V. Filippenko, *Astrophys. J.*, 2008, 685(2): 752, arXiv: 0805.4360
42. J. D. Neill, M. Sullivan, D. A. Howell, A. Conley, et al., *Astrophys. J.*, 2009, 707(2): 1449, arXiv: 0911.0690
43. D. A. Howell, M. Sullivan, E. F. Brown, A. Conley, et al., *Astrophys. J.*, 2009, 691(1): 661, arXiv: 0810.0031
44. D. R. Silva and R. Elston, *Astrophys. J.*, 1994, 428: 511
45. G. Worthey, *Astrophys. J. Suppl.*, 1994, 95: 107
46. J. Guy, P. Astier, S. Nobili, N. Regnault, and R. Pain, *Astron. Astrophys.*, 2005, 443(3): 781, arXiv: astro-ph/0506583
47. J. Guy, P. Astier, S. Baumont, D. Hardin, et al., *Astron. Astrophys.*, 2007, 466(1): 11, arXiv: astro-ph/0701828
48. S. Jha, *Exploding Stars, Near and Far*, Ph.D. thesis, Harvard University, 2002
49. S. Jha, A. G. Riess, and R. P. Kirshner, *Astrophys. J.*, 2007, 659(1): 122, arXiv: astro-ph/0612666
50. C. R. Burns, M. Stritzinger, M. M. Phillips, S. Kattner, et al., *Astronom. J.*, 2011, 141: 19, arXiv: 1010.4040 [astro-ph.CO]
51. F. X. Timmes, E. F. Brown, and J. W. Truran, *Astrophys. J.*, 2003, 590(2): L83, arXiv: astro-ph/0305114
52. K. Nomoto, F. K. Thielemann, and K. Yokoi, *Astrophys. J.*, 1984, 286: 644
53. F. Mannucci, M. Della Valle, and N. Panagia, *Mon. Not. R. Astron. Soc.*, 2006, 370: 773, arXiv: astro-ph/0510315
54. C. Raskin, E. Scannapieco, J. Rhoads, and M. D. Valle, *Astrophys. J.*, 2009, 707(1): 74, arXiv: 0909.4293
55. T. D. Brandt, R. Tojeiro, E. Aubourg, A. Heavens, R. Jimenez, and M. A. Strauss, *Astronom. J.*, 2010, 140: 804, arXiv: 1002.0848 [astro-ph.GA]
56. N. Chotard, E. Gangler, G. Aldering, P. Antilogus, et al., *Astron. Astrophys.*, 2011, 529: L4, arXiv: 1103.5300 [astro-ph.CO]
57. D. A. Howell, M. Sullivan, P. E. Nugent, R. S. Ellis, et al., *Nature*, 2006, 443: 308, arXiv: astro-ph/0609616
58. R. A. Scalzo, G. Aldering, P. Antilogus, C. Aragon, et al., *Astrophys. J.*, 2010, 713(2): 1073, arXiv: 1003.2217 [astro-ph.CO]

59. F. Yuan, R. M. Quimby, J. C. Wheeler, J. Vinkó, E. Chatzopoulos, C. W. Akerlof, S. Kulkarni, J. M. Miller, T. A. McKay, and F. Aharonian, *Astrophys. J.*, 2010, 715(2): 1338, arXiv: 1004.3329 [astro-ph.CO]
60. M. Tanaka, K. S. Kawabata, M. Yamanaka, K. Maeda, T. Hattori, K. Aoki, K. Nomoto, M. Iye, T. Sasaki, P. A. Mazzali, and E. Pian, *Astrophys. J.*, 2010, 714(2): 1209, arXiv: 0908.2057 [astro-ph.CO]
61. S. Chandrasekhar, *Astrophys. J.*, 1931, 74: 81
62. S. Chandrasekhar, *Mon. Not. R. Astron. Soc.*, 1935, 95: 207
63. S. Chandrasekhar, *An introduction to the Study of Stellar Structure*, New York: Dover, 1967
64. E. Mörtzell, L. Bergström, and A. Goobar, *Phys. Rev. D*, 2002, 66(4): 047702, arXiv: astro-ph/0202153
65. P. L. Biermann and L. Clavelli, *Phys. Rev. D*, 2011, 84(2): 023001, arXiv: 1011.1687 [astro-ph.HE]
66. M. Livio, in: *Type Ia Supernovae, Theory and Cosmology*, edited by J. C. Niemeyer and J. W. Truran, 2000: 33
67. B. Wang and Z. Han, *New Astron. Rev.*, 2012, 56(4): 122, arXiv: 1204.1155 [astro-ph.SR]
68. D. Branch, A. Fisher, and P. Nugent, *Astron. J.*, 1993, 106: 2383
69. M. Stritzinger, P. A. Mazzali, J. Sollerman, and S. Benetti, *Astron. Astrophys.*, 2006, 460: 793, arXiv: astro-ph/0609232
70. W. Li, J. Leaman, R. Chornock, A. V. Filippenko, D. Poznanski, M. Ganeshalingam, X. Wang, M. Modjaz, S. Jha, R. J. Foley, and N. Smith, *Mon. Not. R. Astron. Soc.*, 2011, 412(3): 1441, arXiv: 1006.4612 [astro-ph.SR]
71. R. J. Foley, P. J. Challis, R. Chornock, M. Ganeshalingam, et al., arXiv: 1212.2209 [astro-ph.SR], 2012
72. E. Müller, in: *Late Stages of Stellar Evolution. Computational Methods in Astrophysical Hydrodynamics*, Lecture Notes in Physics, Vol. 373, edited by C. B. De Loore, Berlin: Springer-Verlag, 1991: 97
73. L. R. Yungelson and M. Livio, *Astrophys. J.*, 2000, 528(1): 108, arXiv: astro-ph/9907359
74. B. Wang, X. D. Li, and Z. W. Han, *Mon. Not. R. Astron. Soc.*, 2010, 401(4): 2729, arXiv: 0910.2138 [astro-ph.SR]
75. A. J. Ruiter, K. Belczynski, and C. Fryer, *Astrophys. J.*, 2009, 699(2): 2026, arXiv: 0904.3108 [astro-ph.SR]
76. A. J. Ruiter, K. Belczynski, S. A. Sim, W. Hillebrandt, C. L. Fryer, M. Fink, and M. Kromer, *Mon. Not. R. Astron. Soc.*, 2011, 417(1): 408, arXiv: 1011.1407 [astro-ph.SR]
77. E. Bravo, L. Piersanti, I. Domínguez, O. Straniero, J. Isern, and J. A. Escartin, *Astron. Astrophys.*, 2011, 535: A114, arXiv: 1110.1949 [astro-ph.SR]
78. J. Whelan and I. Iben, Jr., *Astrophys. J.*, 1973, 186: 1007
79. I. Hachisu, M. Kato, and K. Nomoto, *Astrophys. J.*, 1996, 470(2): L97
80. Z. Han and P. Podsiadlowski, *Mon. Not. R. Astron. Soc.*, 2004, 350(4): 1301, arXiv: astro-ph/0309618
81. B. Wang and Z.W. Han, *Res. Astron. Astrophys.*, 2010, 10: 235, arXiv: 1003.4568 [astro-ph.SR]
82. B. Wang, X. Meng, X. Chen, and Z. Han, *Mon. Not. R. Astron. Soc.*, 2009, 395(2): 847, arXiv: 0901.3496 [astro-ph.SR]
83. D. Kasen, *Astrophys. J.*, 2010, 708(2): 1025, arXiv: 0909.0275 [astro-ph.HE]
84. P. E. Nugent, M. Sullivan, S. B. Cenko, R. C. Thomas, et al., *Nature*, 2011, 480(7377): 344, arXiv: 1110.6201 [astro-ph.CO]
85. P. J. Brown, K. S. Dawson, M. de Pasquale, C. Gronwall, S. Holland, S. Immler, P. Kuin, P. Mazzali, P. Milne, S. Oates, and M. Siegel, *Astrophys. J.*, 2012, 753(1): 22, arXiv: 1110.2538 [astro-ph.CO]
86. W. Li, J. S. Bloom, P. Podsiadlowski, A. A. Miller, et al., *Nature*, 2011, 480(7377): 348, arXiv: 1109.1593 [astro-ph.CO]
87. J. C. Wheeler, *Astrophys. J.*, 2012, 758(2): 123, arXiv: 1209.1021 [astro-ph.SR]
88. B. Dilday, D. A. Howell, S. B. Cenko, J. M. Silverman, et al., *Science*, 2012, 337(6097): 942, arXiv: 1207.1306 [astro-ph.CO]
89. P. A. Mazzali, D. N. Sauer, A. Pastorello, S. Benetti, and W. Hillebrandt, *Mon. Not. R. Astron. Soc.*, 2008, 386(4): 1897, arXiv: 0803.1383
90. W. D. Arnett, *Astrophys. Space Sci.*, 1969, 5(2): 180
91. F. K. Röpkke, W. Hillebrandt, W. Schmidt, J. C. Niemeyer, S. I. Blinnikov, and P. A. Mazzali, *Astrophys. J.*, 2007, 668(2): 1132, arXiv: 0707.1024
92. A. M. Khokhlov, *Astron. Astrophys.*, 1991, 245: 114
93. P. Höflich, A. M. Khokhlov, and J. C. Wheeler, *Astrophys. J.*, 1995, 444: 831
94. P. Höflich and A. Khokhlov, *Astrophys. J.*, 1996, 457: 500, arXiv: astro-ph/9602025
95. D. Arnett and E. Livne, *Astrophys. J.*, 1994, 427: 315
96. D. Arnett and E. Livne, *Astrophys. J.*, 1994, 427: 330
97. T. Plewa, A. C. Calder, and D. Q. Lamb, *Astrophys. J.*, 2004, 612(1): L37
98. G. C. IV Jordan, R. T. Fisher, D. M. Townsley, A. C. Calder, C. Graziani, S. Asida, D. Q. Lamb, and J. W. Truran, *Astrophys. J.*, 2008, 681(2): 1448, arXiv: astro-ph/0703573
99. I. R. Seitenzahl, C. A. Meakin, D. Q. Lamb, and J. W. Truran, *Astrophys. J.*, 2009, 700(1): 642, arXiv: 0905.3104 [astro-ph.SR]
100. D. A. Chamulak, C. A. Meakin, I. R. Seitenzahl, and J. W. Truran, *Astrophys. J.*, 2012, 744(1): 27, arXiv: 1103.3062 [astro-ph.SR]
101. S. I. Blinnikov and A. M. Khokhlov, *Sov. Astron. Lett.*, 1986, 12: 131
102. S. E. Woosley, in: *Supernovae*, edited by A. G. Petschek, 1990: 182
103. A. M. Khokhlov, E. S. Oran, and J. C. Wheeler, *Astrophys. J.*, 1997, 478(2): 678, arXiv: astro-ph/9612226
104. J. C. Niemeyer and S. E. Woosley, *Astrophys. J.*, 1997, 475(2): 740, arXiv: astro-ph/9607032
105. P. Höflich, J. C. Wheeler, and F. K. Thielemann, *Astrophys. J.*, 1998, 495: 617, arXiv: astro-ph/9709233
106. J. C. Niemeyer, *Astrophys. J.*, 1999, 523(1): L57, arXiv: astro-ph/9906142

107. K. Maeda, S. Benetti, M. Stritzinger, F. K. Röpke, G. Folatelli, J. Sollerman, S. Taubenberger, K. Nomoto, G. Leloudas, M. Hamuy, M. Tanaka, P. A. Mazzali, and N. Elias-Rosa, *Nature*, 2010, 466(7302): 82, arXiv: 1006.5888 [astro-ph.CO]
108. A. V. Tutukov and L. R. Iungelson, *Astrofizika*, 1976, 12: 521
109. A. V. Tutukov and L. R. Yungelson, *Acta Astronaut.*, 1979, 29: 665
110. R. F. Webbink, *Astrophys. J.*, 1984, 277: 355
111. I. Iben, Jr. and A. V. Tutukov, *Astrophys. J. Suppl.*, 1984, 54: 335
112. H. Saio and K. Nomoto, *Astron. Astrophys.*, 1985, 150: L21
113. H. Saio and K. Nomoto, *Astrophys. J.*, 2004, 615(1): 444, arXiv: astro-ph/0401141
114. K. Nomoto and Y. Kondo, *Astrophys. J.*, 1991, 367: L19
115. Y. Kawai, H. Saio, and K. Nomoto, *Astrophys. J.*, 1987, 315: 229
116. R. Pakmor, S. Hachinger, F. K. Röpke, and W. Hillebrandt, *Astron. Astrophys.*, 2011, 528: A117, arXiv: 1102.1354 [astro-ph.SR]
117. S. Rosswog, D. Kasen, J. Guillochon, and E. Ramirez-Ruiz, *Astrophys. J.*, 2009, 705(2): L128, arXiv: 0907.3196 [astro-ph.HE]
118. C. Raskin, F. X. Timmes, E. Scannapieco, S. Diehl, and C. Fryer, *Mon. Not. R. Astron. Soc.*, 2009, 399(1): L156, arXiv: 0907.3915 [astro-ph.SR]
119. C. Raskin, E. Scannapieco, G. Rockefeller, C. Fryer, S. Diehl, and F. X. Timmes, *Astrophys. J.*, 2010, 724(1): 111, arXiv: 1009.2507 [astro-ph.SR]
120. P. Lorén-Aguilar, J. Isern, and E. García-Berro, *Mon. Not. R. Astron. Soc.*, 2010, 406(4): 2749, arXiv: 1004.4783 [astro-ph.SR]
121. X. Meng and W. Yang, *Astron. Astrophys.*, 2012, 543: A137, arXiv: 1205.2452 [astro-ph.SR]
122. W. Benz, A. G. W. Cameron, W. H. Press, and R. L. Bowers, *Astrophys. J.*, 1990, 348: 647
123. S. C. Yoon, P. Podsiadlowski, and S. Rosswog, *Mon. Not. R. Astron. Soc.*, 2007, 380(3): 933, arXiv: 0704.0297
124. P. Lorén-Aguilar, J. Isern, and E. García-Berro, *Astron. Astrophys.*, 2009, 500(3): 1193
125. K. J. Shen, L. Bildsten, D. Kasen, and E. Quataert, *Astrophys. J.*, 2012, 748(1): 35
126. C. L. Fryer and S. Diehl, in: *Hydrogen-Deficient Stars*, Astronomical Society of the Pacific Conference Series, Vol. 391, edited by A. Werner and T. Rauch, 2008: 335, arXiv: 0711.0864
127. S. Diehl, C. Fryer, A. Hungerford, G. Rockefeller, M. E. Ben-net, F. Herwig, R. Hirschi, M. Pignatari, G. Magkotsios, F. X. Timmes, P. Young, G. C. Clayton, P. Motl, and J. E. Tohline, in: *Nuclei in the Cosmos (NIC X)*, 2008
128. M. C. R. D'Souza, P. M. Motl, J. E. Tohline, and J. Frank, *Astrophys. J.*, 2006, 643: 381, arXiv: astro-ph/0512137
129. P. M. Motl, J. Frank, J. E. Tohline, and M. C. R. D'Souza, *Astrophys. J.*, 2007, 670: 1314, arXiv: astro-ph/0702388
130. M. Dan, S. Rosswog, J. Guillochon, and E. Ramirez-Ruiz, *Astrophys. J.*, 2011, 737(2): 89, arXiv: 1101.5132 [astro-ph.HE]
131. M. Dan, S. Rosswog, J. Guillochon, and E. Ramirez-Ruiz, *Mon. Not. R. Astron. Soc.*, 2012, 422(3): 2417, arXiv: 1201.2406 [astro-ph.HE]
132. R. Pakmor, P. Edelmann, F. K. Röpke, and W. Hillebrandt, arXiv: 1205.5806 [astro-ph.HE], 2012
133. R. Pakmor, M. Kromer, F. K. Röpke, S. A. Sim, A. J. Ruiter, and W. Hillebrandt, *Nature*, 2010, 463(7277): 61, arXiv: 0911.0926 [astro-ph.HE]
134. R. Pakmor, M. Kromer, S. Taubenberger, S. A. Sim, F. K. Röpke, and W. Hillebrandt, *Astrophys. J.*, 2012, 747(1): L10, arXiv: 1201.5123 [astro-ph.HE]
135. M. Steinmetz, E. Muller, and W. Hillebrandt, *Astron. Astrophys.*, 1992, 254: 177
136. J. M. M. Pfannes, J. C. Niemeyer, W. Schmidt, and C. Klingenberg, *Astron. Astrophys.*, 2010, 509: A74, arXiv: 0911.3540 [astro-ph.HE]
137. J. M. M. Pfannes, J. C. Niemeyer, and W. Schmidt, *Astron. Astrophys.*, 2010, 509: A75, arXiv: 0911.3545 [astro-ph.HE]
138. I. Hachisu, M. Kato, H. Saio, and K. Nomoto, *Astrophys. J.*, 2012, 744(1): 69, arXiv: 1106.3510 [astro-ph.SR]
139. S. E. Woosley, T. A. Weaver, and R. E. Taam, in: *Texas Workshop on Type I Supernovae*, edited by J. C. Wheeler, 1980: 96
140. R. E. Taam, *Astrophys. J.*, 1980, 237: 142
141. R. E. Taam, *Astrophys. J.*, 1980, 242: 749
142. K. Nomoto, *Space Sci. Rev.*, 1980, 27(3–4): 563
143. K. Nomoto, *Astrophys. J.*, 1982, 257: 780
144. E. Livne, *Astrophys. J.*, 1990, 354: L53
145. S. E. Woosley and T. A. Weaver, *Astrophys. J.*, 1994, 423: 371
146. E. Livne and A. S. Glasner, *Astrophys. J.*, 1991, 370: 272
147. E. Livne and D. Arnett, *Astrophys. J.*, 1995, 452: 62
148. P. Hoeflich, A. Khokhlov, J. C. Wheeler, M. M. Phillips, N. B. Suntzeff, and M. Hamuy, *Astrophys. J.*, 1996, 472: L81, arXiv: astro-ph/9609070
149. D. J. R. Wiggins and S. A. E. G. Falle, *Mon. Not. R. Astron. Soc.*, 1997, 287: 575
150. D. J. R. Wiggins, G. J. Sharpe, and S. A. E. G. Falle, *Mon. Not. R. Astron. Soc.*, 1998, 301(2): 405
151. D. García-Senz, E. Bravo, and S. E. Woosley, *Astron. Astrophys.*, 1999, 349: 177
152. M. Fink, W. Hillebrandt, and F. K. Röpke, *Astron. Astrophys.*, 2007, 476(3): 1133, arXiv: 0710.5486
153. S. A. Sim, F. K. Röpke, W. Hillebrandt, M. Kromer, R. Pakmor, M. Fink, A. J. Ruiter, and I. R. Seitenzahl, *Astrophys. J.*, 2010, 714(1): L52, arXiv: 1003.2917 [astro-ph.HE]
154. L. Bildsten, K. J. Shen, N. N. Weinberg, and G. Nelemans, *Astrophys. J. Lett.*, 2007, 662: L95, arXiv: astro-ph/0703578
155. M. Fink, F. K. Röpke, W. Hillebrandt, I. R. Seitenzahl, S. A. Sim, and M. Kromer, *Astron. Astrophys.*, 2010, 514: A53, arXiv: 1002.2173 [astro-ph.SR]

156. M. Kromer, S. A. Sim, M. Fink, F. K. Röpke, I. R. Seitenzahl, and W. Hillebrandt, *Astrophys. J.*, 2010, 719(2): 1067, arXiv: 1006.4489 [astro-ph.HE]
157. S. E. Woosley and D. Kasen, *Astrophys. J.*, 2011, 734(1): 38, arXiv: 1010.5292 [astro-ph.HE]
158. S. A. Sim, M. Fink, M. Kromer, F. K. Röpke, A. J. Ruiter, and W. Hillebrandt, *Mon. Not. R. Astron. Soc.*, 2012, 420(4): 3003, arXiv: 1111.2117 [astro-ph.HE]
159. K. Nomoto, *Astrophys. J.*, 1982, 253: 798
160. S. E. Woosley and T. A. Weaver, *Annu. Rev. Astron. Astrophys.*, 1986, 24(1): 205
161. A. Nonaka, A. J. Aspden, M. Zingale, A. S. Almgren, J. B. Bell, and S. E. Woosley, *Astrophys. J.*, 2012, 745(1): 73, arXiv: 1111.3086 [astro-ph.HE]
162. A. L. Piro and L. Bildsten, *Astrophys. J.*, 2008, 673(2): 1009, arXiv: 0710.1600
163. F. K. Röpke, *Astrophys. J.*, 2007, 668(2): 1103, arXiv: 0709.4095
164. I. R. Seitenzahl, C. A. Meakin, D. M. Townsley, D. Q. Lamb, and J. W. Truran, *Astrophys. J.*, 2009, 696(1): 515, arXiv: 0901.3677
165. S. E. Woosley, A. R. Kerstein, V. Sankaran, A. J. Aspden, and F. K. Röpke, *Astrophys. J.*, 2009, 704(1): 25, arXiv: 0811.3610
166. W. Schmidt, F. Ciaraldi-Schoolmann, J. C. Niemeyer, F. K. Röpke, and W. Hillebrandt, *Astrophys. J.*, 2010, 710(2): 1683, arXiv: 0911.4345
167. A. Y. Poludnenko, T. A. Gardiner, and E. S. Oran, *Phys. Rev. Lett.*, 2011, 107(5): 054501, arXiv: 1106.3696 [astro-ph.HE]
168. C. Charignon and J. P. Chièze, arXiv: 1301.1523 [astro-ph.HE], 2013
169. S. B. Pope, *Ann. Rev. Fluid Mech.*, 1987, 19(1): 237
170. I. Golombek and J. C. Niemeyer, *Astron. Astrophys.*, 2005, 438(2): 611, arXiv: astro-ph/0503617
171. F. K. Röpke and W. Hillebrandt, *Astron. Astrophys.*, 2005, 429: L29, arXiv: astro-ph/0411667
172. A. J. Aspden, J. B. Bell, M. S. Day, S. E. Woosley, and M. Zingale, *Astrophys. J.*, 2008, 689(2): 1173, arXiv: 0811.2816
173. A. J. Aspden, J. B. Bell, and S. E. Woosley, *Astrophys. J.*, 2010, 710(2): 1654
174. A. Y. Poludnenko and E. S. Oran, *Combust. Flame*, 2011, 157(5): 995
175. A. Y. Poludnenko and E. S. Oran, *Combust. Flame*, 2011, 158(2): 301
176. S. E. Woosley, *Astrophys. J.*, 2007, 668(2): 1109, arXiv: 0709.4237
177. A. M. Lisewski, W. Hillebrandt, and S. E. Woosley, *Astrophys. J.*, 2000, 538(2): 831, arXiv: astro-ph/9910056
178. F. K. Röpke and J. C. Niemeyer, *Astron. Astrophys.*, 2007, 464(2): 683, arXiv: astro-ph/0703378
179. E. Bravo and D. García-Senz, *Astron. Astrophys.*, 2008, 478(3): 843, arXiv: 0712.0510
180. K. Maeda, F. K. Röpke, M. Fink, W. Hillebrandt, C. Travaglio, and F. K. Thielemann, *Astrophys. J.*, 2010, 712(1): 624, arXiv: 1002.2153 [astro-ph.SR]
181. A. P. Jackson, A. C. Calder, D. M. Townsley, D. A. Chamulak, E. F. Brown, and F. X. Timmes, *Astrophys. J.*, 2010, 720(1): 99, arXiv: 1007.1138 [astro-ph.SR]
182. O. Straniero, I. Domínguez, G. Imbriani, and L. Piersanti, *Astrophys. J.*, 2003, 583: 878, arXiv: astro-ph/0210191
183. H. Umeda, K. Nomoto, H. Yamaoka, and S. Wanaajo, *Astrophys. J.*, 1999, 513(2): 861
184. D. A. Chamulak, E. F. Brown, F. X. Timmes, and K. Dupczak, *Astrophys. J.*, 2008, 677(1): 160
185. D. Branch, M. Livio, L. R. Yungelson, F. R. Boffi, and E. Baron, *Publ. Astron. Soc. Pac.*, 1995, 107: 1019
186. L. R. Gasques, A. V. Afanasjev, E. F. Aguileria, M. Beard, L. C. Chamon, P. Ring, M. Wiescher, and D. G. Yakovlev, *Phys. Rev. C*, 2005, 72: 025806, arXiv: astro-ph/0506386
187. D. G. Yakovlev, L. R. Gasques, A. V. Afanasjev, M. Beard, and M. Wiescher, *Phys. Rev. C*, 2006, 74(3): 035803, arXiv: astro-ph/0608488
188. A. C. Calder, D. M. Townsley, I. R. Seitenzahl, F. Peng, O. E. B. Messer, N. Vladimirova, E. F. Brown, J. W. Truran, and D. Q. Lamb, *Astrophys. J.*, 2007, 656(1): 313, arXiv: astro-ph/0611009
189. F. X. Timmes and S. E. Woosley, *Astrophys. J.*, 1992, 396: 649
190. D. A. Chamulak, E. F. Brown, and F. X. Timmes, *Astrophys. J.*, 2007, 655(2): L93, arXiv: astro-ph/0612507
191. J. C. Niemeyer and W. Hillebrandt, *Astrophys. J.*, 1995, 452: 769
192. M. Zingale and L. J. Dursi, *Astrophys. J.*, 2007, 656(1): 333, arXiv: astro-ph/0610297
193. E. Bravo, J. Isern, R. Canal, and J. Labay, *Astron. Astrophys.*, 1992, 257: 534
194. L. G. Althaus, E. García-Berro, I. Renedo, J. Isern, A. H. Córscico, and R. D. Rohrmann, *Astrophys. J.*, 2010, 719(1): 612, arXiv: 1006.4170 [astro-ph.SR]
195. E. Bravo, L. G. Althaus, E. García-Berro, and I. Domínguez, *Astron. Astrophys.*, 2011, 526: A26, arXiv: 1010.5098 [astro-ph.SR]
196. D. Kasen, F. K. Röpke, and S. E. Woosley, *Nature*, 2009, 460(7257): 869, arXiv: 0907.0708 [astro-ph.HE]
197. P. Höflich, J. C. Wheeler, and F. K. Thielemann, *Astrophys. J.*, 1998, 495(2): 617, arXiv: astro-ph/9709233
198. H. Umeda, K. Nomoto, C. Kobayashi, I. Hachisu, and M. Kato, *Astrophys. J.*, 1999, 522(1): L43
199. F. K. Röpke and W. Hillebrandt, *Astron. Astrophys.*, 2004, 420: L1, arXiv: astro-ph/0403509
200. E. Bravo, I. Domínguez, C. Badenes, L. Piersanti, and O. Straniero, *Astrophys. J.*, 2010, 711(2): L66, arXiv: 1002.0681
201. C. Contreras, M. Hamuy, M. M. Phillips, G. Folatelli, et al., *Astronom. J.*, 2010, 139: 519, arXiv: 0910.3330 [astro-ph.CO]
202. G. Folatelli, M. M. Phillips, C. R. Burns, C. Contreras, et al., *Astronom. J.*, 2010, 139: 120, arXiv: 0910.3317 [astro-ph.CO]



203. P. Höflich and J. Stein, *Astrophys. J.*, 2002, 568(2): 779, arXiv: astro-ph/0104226
204. S. E. Woosley, S. Wunsch, and M. Kuhlen, *Astrophys. J.*, 2004, 607(2): 921, arXiv: astro-ph/0307565
205. M. Kuhlen, S. E. Woosley, and G. A. Glatzmaier, *Astrophys. J.*, 2006, 640(1): 407, arXiv: astro-ph/0509367
206. A. L. Piro and P. Chang, *Astrophys. J.*, 2008, 678(2): 1158, arXiv: 0801.1321
207. M. Zingale, A. S. Almgren, J. B. Bell, A. Nonaka, and S. E. Woosley, *Astrophys. J.*, 2009, 704(1): 196, arXiv: 0908.2668
208. M. Zingale, A. Nonaka, A. S. Almgren, J. B. Bell, C. M. Malone, and S. E. Woosley, *Astrophys. J.*, 2011, 740(1): 8
209. C. L. Jiang, K. E. Rehm, B. B. Back, and R. V. F. Janssens, *Phys. Rev. C*, 2007, 75(1): 015803
210. R. L. Cooper, A. W. Steiner, and E. F. Brown, *Astrophys. J.*, 2009, 702(1): 660, arXiv: 0903.3994 [astro-ph.HE]
211. L. Iapichino and P. Lesaffre, *Astron. Astrophys.*, 2010, 512: A27, arXiv: 1001.2165 [astro-ph.SR]
212. B. Paczyński, *Astrophys. Lett.*, 1972, 11: 53
213. I. Iben, Jr., *Astrophys. J.*, 1978, 219: 213
214. I. Iben, Jr., *Astrophys. J.*, 1978, 226: 996
215. I. Iben, Jr., *Astrophys. J.*, 1982, 253: 248
216. J. Stein, Z. Barkat, and J. C. Wheeler, *Astrophys. J.*, 1999, 523(1): 381
217. P. Lesaffre, P. Podsiadlowski, and C. A. Tout, *Mon. Not. R. Astron. Soc.*, 2005, 356(1): 131
218. E. Bravo, J. Isern, R. Canal, and J. Labay, *Astrophys. Space Sci.*, 1990, 169(1–2): 19
219. R. Fisher, D. Falta, G. Jordan, and D. Lamb, in: *Gravitation and Astrophysics*, edited by J. Luo, Z.-B. Zhou, H.-C. Yeh, and J.-P. Hsu, 2010: 335–344, arXiv: 1005.0026 [astro-ph.SR]
220. I. R. Seitenzahl, F. Ciaraldi-Schoolmann, F. K. Röpke, M. Fink, W. Hillebrandt, M. Kromer, R. Pakmor, A. J. Ruiter, S. A. Sim, and S. Taubenberger, *Mon. Not. R. Astron. Soc.*, 2013, 429(2): 1156, arXiv: 1211.3015 [astro-ph.SR]
221. F. K. Röpke and J. C. Niemeyer, *Astron. Astrophys.*, 2007, 464(2): 683 arXiv: astro-ph/0703378
222. B. Fryxell, K. Olson, P. Ricker, F. X. Timmes, M. Zingale, D. Q. Lamb, P. MacNeice, R. Rosner, J. W. Truran, and H. Tufo, *Astrophys. J. Suppl.*, 2000, 131(1): 273
223. A. C. Calder, B. C. Curtis, L. J. Dursi, B. Fryxell, G. Henry, P. MacNeice, K. Olson, P. Ricker, R. Rosner, F. X. Timmes, H. M. Tufo, J. W. Truran, and M. Zingale, in: *Proceedings of Supercomputing 2000*, 2000, <http://sc2000.org>
224. A. C. Calder, B. Fryxell, T. Plewa, R. Rosner, et al., *Astrophys. J. Suppl.*, 2002, 143(1): 201
225. E. F. Brown, A. C. Calder, T. Plewa, P. M. Ricker, K. Robinson, and J. B. Gallagher, *Nucl. Phys. A.*, 2005, 758: 451, arXiv: astro-ph/0505417
226. D. M. Townsley, F. X. Timmes, A. P. Jackson, A. C. Calder, and E. F. Brown, *Astrophys. J.*, 2012 (to be submitted)
227. D. M. Townsley, A. C. Calder, S. M. Asida, I. R. Seitenzahl, F. Peng, N. Vladimirova, D. Q. Lamb, and J. W. Truran, *Astrophys. J.*, 2007, 668(2): 1118, arXiv: 0706.1094
228. A. M. Khokhlov, *Astrophys. J.*, 1995, 449: 695
229. N. Vladimirova, G. Weirs, and L. Ryzhik, *Combust. Theory Modeling*, 2006, 10(5): 727
230. F. X. Timmes and S. E. Woosley, *Astrophys. J.*, 1992, 396: 649
231. G. Taylor, *Royal Society of London Proceedings Series A*, 1950, 201(1065): 192
232. S. Chandrasekhar, *Hydrodynamic and Hydromagnetic Stability*, New York: Dover, 1981
233. D. Townsley, *Comput. Sci. Eng.*, 2009, 11(2): 18
234. V. N. Gamezo, A. M. Khokhlov, E. S. Oran, A. Y. Chtchelkanova, and R. O. Rosenberg, *Science*, 2003, 299(5603): 77
235. A. P. Jackson, D. M. Townsley, and A. C. Calder, 2012 (in preparation)
236. D. Bodansky, D. D. Clayton, and W. A. Fowler, *Astrophys. J. Suppl.*, 1968, 16: 299
237. S. E. Woosley, W. D. Arnett, and D. D. Clayton, *Astrophys. J. Suppl.*, 1973, 26: 231
238. V. S. Imshennik, S. S. Filippov, and A. M. Khokhlov, *Sov. Astron. Lett.*, 1981, 7: 121
239. A. M. Khokhlov, *Sov. Astron. Lett.*, 1981, 7: 410
240. A. M. Khokhlov, *Sov. Astron. Lett.*, 1983, 9: 160
241. K. Langanke and G. Martínez-Pinedo, *At. Data Nucl. Data Tables*, 2001, 79(1): 1
242. I. R. Seitenzahl, D. M. Townsley, F. Peng, and J. W. Truran, *At. Data Nucl. Data Tables*, 2009, 95(1): 96
243. C. A. Meakin, I. Seitenzahl, D. Townsley, G. C. Jordan, J. Truran, and D. Lamb, *Astrophys. J.*, 2009, 693(2): 1188, arXiv: 0806.4972
244. V. N. Gamezo, A. M. Khokhlov, and E. S. Oran, *Astrophys. J.*, 2005, 623(1): 337, arXiv: astro-ph/0409598
245. A. M. Khokhlov, arXiv: astro-ph/0008463, 2000
246. K. Konishi, D. Cinabro, P. M. Garnavich, Y. Ihara, R. Kessler, J. Marriner, D. P. Schneider, M. Smith, H. Spinka, J. C. Wheeler, and N. Yasuda, arXiv: 1101.4269 [astro-ph.CO], 2011
247. B. Carroll and D. Ostlie, *An Introduction to Modern Astrophysics*, Pearson Addison-Wesley, 2007
248. B. K. Krueger, A. P. Jackson, D. M. Townsley, A. C. Calder, E. F. Brown, and F. X. Timmes, *Astrophys. J. Lett.*, 2010, 719: L5, arXiv: 1007.0910
249. B. K. Krueger, A. P. Jackson, A. C. Calder, D. M. Townsley, E. F. Brown, and F. X. Timmes, *Astrophys. J.*, 2012, 757(2): 175
250. G. Goldhaber, D. E. Groom, A. Kim, G. Aldering, et al., *Astrophys. J.*, 2001, 558: 359, arXiv: astro-ph/0104382
251. C. J. Hansen, S. D. Kawaler, and V. Trimble, *Stellar interiors: Physical Principles, Structure, and Evolution*, New York: Springer-Verlag, 2004